Hybrid Laser Welding of Large Steel Structures

An Experimental and Numerical Study

Farrokhi, Farhang

DOI (link to publication from Publisher):
10.5278/VBN.PHD.ENG.00038

Publication date:
2018

Document Version
Publisher's PDF, also known as Version of record

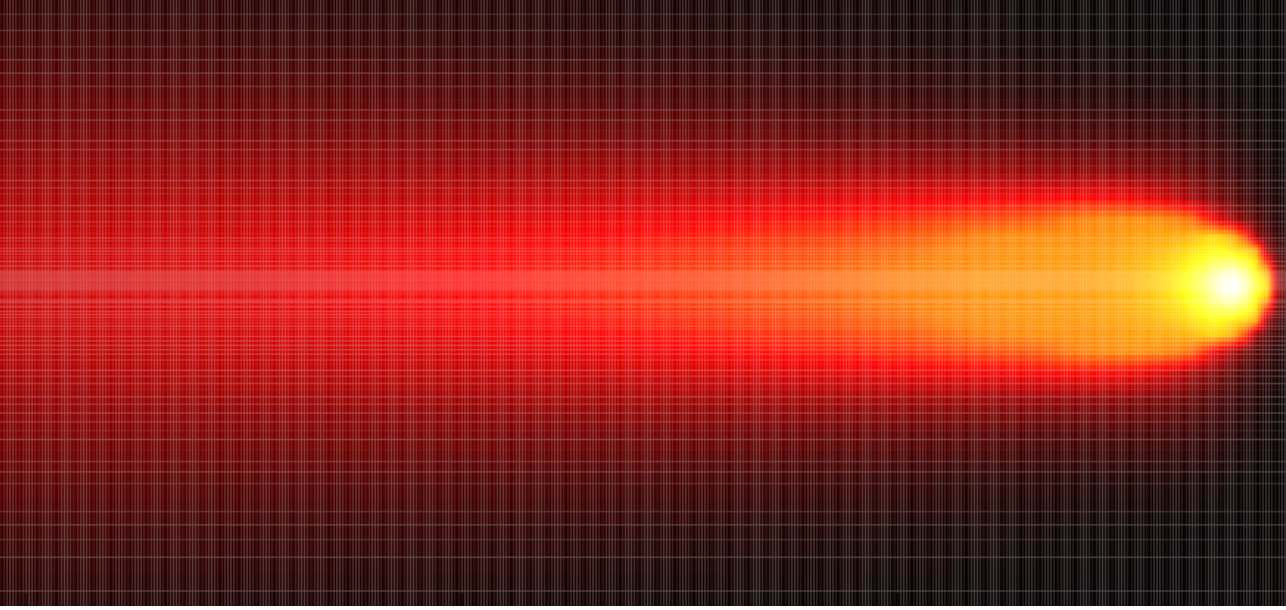

HYBRID LASER WELDING OF LARGE STEEL STRUCTURES

AN EXPERIMENTAL AND NUMERICAL STUDY

BY
FARHANG FARROKHI

DISSERTATION SUBMITTED 2018

AALBORG UNIVERSITY
DENMARK

Hybrid Laser Welding of Large Steel Structures:

An Experimental and Numerical Study

Ph.D. Dissertation

Farhang Farrokhi

Dissertation submitted February 26, 2018

Dissertation submitted: February 26, 2018

PhD supervisor: Associate Professor Morten Kristiansen
Aalborg University

PhD committee: Associate Professor Jens H. Andreasen (chairman)
Aalborg University

Associate Professor Jan Frostevarg
Luleå University of Technology

Adjunct Professor Jens Klæstrup Kristensen
Technical University of Denmark

PhD Series: Faculty of Engineering and Science, Aalborg University

Department: Department of Materials and Production

ISSN (online): 2446-1636
ISBN (online): 978-87-7210-163-7

Published by:
Aalborg University Press
Langagervej 2
DK – 9220 Aalborg Ø
Phone: +45 99407140
aauf@forlag.aau.dk
forlag.aau.dk

Printed in Denmark by Rosendahls, 2018

In memory of my only brother

Fardad Farrokhi.

Abstract

Manufacturing of large steel structures, e.g. offshore wind turbine foundations, requires the processing of thick-section steels. Welding is one of the main operations during the manufacturing of such structures and includes a significant part of the production costs. One of the ways to reduce the production costs is to use the hybrid laser welding technology instead of the conventional arc welding methods. However, hybrid laser welding is a complicated process that involves several complex physical phenomena that are highly coupled. Understanding of the process is very important for obtaining quality welds efficiently.

This thesis, investigates two different challenges related to the hybrid laser welding of thick-section steel plates; (i) Integration of laser cutting and welding processes in the same unit in order to increase the productivity; (ii) Avoidance of solidification cracking that often occurs in the deep laser welds of steel.

To address the first challenge, a number of experiments were carried out. The experiments investigated the influence of laser cutting as the preparation method, compared with the different conventional preparation techniques in industry, on the quality and efficiency of the subsequent hybrid laser welding. Two characteristics of laser cut surfaces, (i) roughness and (ii) perpendicularity were investigated in the comparison. The results were evident that, using laser cutting as preparation method, not only increased the travel speed in the subsequent welding, but also enhanced the stability of the weld root.

Concerning the challenge of weld solidification cracking, the study was focused on the effect of penetration-mode during welding. A number of full and partial penetration welding experiments were carried out and the experiments were modeled using the Finite Element method. The results of experiments showed that partial penetration welding could significantly increase the risk of weld solidification cracking for the given process parameters. The results of numerical modeling also showed that, for the same process parameters, partial penetration welding has a lower tendency for the formation of the advantageous equiaxed grains in the weld centerline, compared with the full penetration welding. Using the numerical model, the formation of the equiaxed microstructure in some full penetration welds could partly be attributed to the extention of the constitutional supercooling region in front of the solid liquid interface. Finally, the study proposed crack-free welding procedures and suggested general guidelines for the avoidance of such cracks in the weld. It was concluded that, in order to reduce the risk of solidification cracking in the hybrid laser welding of thick-section steels, partial penetration welding must be avoided.

Resumé

Fremstilling af store stålkonstruktioner, for eksempel fundamenter til offshore vindmøller, kræver bearbejdning af tykke stålsektioner. Svejsning er en af hovedoperationerne når man fremstiller sådanne sektioner, og den udgør en væsentlig del af produktionsomkostningen. En måde at reducere produktionsomkostningen er, at bruge hybrid lasersvejseteknologi i stedet for de konventionelle lysbuesvejsningsmetoder. Hybrid lasersvejsning er imidlertid en kompliceret proces, der involverer adskillige komplekse fysiske fænomener, som er stærkt koblet. Forståelsen af denne proces er derfor meget vigtig for effektivt at opnå kvalitetssvejsninger.

Denne afhandling undersøger to forskellige udfordringer som er relateret til hybrid lasersvejsning af stålplader i tykke sektioner; (i) Integration af laserskærings og lasersvejsningsprocesser i same enhed for at øge produktiviteten; (ii) Forhindre størkningsrevner, som ofte forekommer ved de dybe lasersvejsninger i stål.

Den første udfordring blev adresseret ved at udføre et antal af eksperimenter. Eksperimenterne undersøgte hvordan laserskæring som forberedelsesmetode, sammenlignet med forskellige konventionelle forberedelsesmetoder brugt i industrien, påvirkede kvaliteten og effektiviteten af den efterfølgende hybride lasersvejsning. To karakteristikker af laserskåret overflader, (i) overfladeruhed og (ii) vinkelrethed, blev undersøgt i sammenligningen. Resultaterne viste at brugen af laserskæring som forberedelsesmetode, ikke kun øgede den efterfølgende svejsehastighed, men også forbedrede stabiliteten af rodsvejsningen.

Hvad angår udfordringen med størkningsrevner, var studiet fokuseret på effekter af gennembrændingsformen under svejsning. Et antal af fuld- og delvisgennembrændings svejsningseksperimenter blev udført og eksperimenterne var modelleret ved brug af Finite Element metoden. Resultaterne fra eksperimenterne viste at delvis gennembrænding kunne øge risikoen for størkningsrevner væsentligt for de givne procesparametre. Resultaterne fra den numeriske modellering har også vist, at for de samme procesparametre, har delvis gennembrændingssvejsninger lavere tendens til dannelse af de fordelagtige ligeaksede kornstrukturer i svejsningens centerlinje sammenlignet med fuld gennembrændingssvejsning. Ved brug af den numeriske model, kan man delvis tilskrive forekomsten af ligeaksede kornstrukture, i nogle fuldgennembrændingssvejsninger, ved en udvidelse af det konstitutionel underafkøling område foran den faste flydegrænse. Endelig, har studiet foreslået nogle procedurer til revne-fri svejsning og også nogle generelle retningslinjer til hvordan sådanne revner i

svejsninger undgås. Det var konkluderet, at for at reducere risikoen for størkningsrevner i hybride lasersvejsninger for tykke stålplader, så skal man, hvis muligt, undgå at lave svejsninger med delvis gennembrændinger.

Contents

Nomenclature

Some of the parameters in the following tables and in the entire thesis may not follow a consistent unit system and are only for presentation. However, for the entire numerical calculations, the unit system (b) was used according to LS-DYNA manual, LSTC [2015].

Greek symbols

α	Angle between the welding direction and the normal direction of the solidification front
β_a	Arc heat partition factor
β_l	Laser heat partition factor
Δs	Numerical element size
Δt	Numerical time step size
ϵ	Emissivity
η_a	Arc heat efficiency
η_l	Laser heat efficiency
λ	Thermal diffusivity
ρ	Density
σ	Stefan-Boltzman constant

Latin symbols

a_h, b_h, c_{hf}, c_{hr}	Geometrical parameters of the double-ellipsoidal heat source
c	Specific heat
D	Plate thickness
D_P	Penetration depth (in Figure 5.6)
$\mathbf{d}$	Depth with respect to the plate top surface
G	Temperature gradient
G_L	Temperature gradient of liquid

$G_{L,av}$	Average temperature gradient of liquid
G_x	Temperature gradient in x direction
G_z	Temperature gradient in z direction
G_{xz}	Temperature gradient on xz plane
h	Convective coefficient
I	Arc current
k	Thermal conductivity
$\mathbf{L}$, $\mathbf{L_A}$, $\mathbf{L_B}$	Dimensions (in Figure 5.2)
L_f	Latent heat of fusion
L_{top}, L_{root}	Melt pool lengths along the welding direction
P_a	Arc power
P_l	Laser power
Q_a	Effective arc power
Q_l	Effective laser power
Q_{l1}	Effective laser power of the lower cone of the double-conical heat source
Q_{l2}	Effective laser power of the upper cone of the double-conical heat source
Q_t	Total effective power
q	Heat flux
q_a	Arc volumetric heat flux
q_c	Heat loss due to convection
q_r	Heat loss due to radiation
q_l	Laser volumetric heat flux
q_v	Total volumetric heat flux
R	Solidification growth rate
R_a	Average surface roughness (two dimensional)
r_f, r_r	Proportional coefficients of the double-ellipsoidal heat source

r_b, r_i, r_t	Radius parameters of the double-conical heat source
r_1	Distribution parameter of the lower cone of the double-conical heat source
r_2	Distribution parameter of the upper cone of the double-conical heat source
S	Penetration depth (in Figure 5.8)
S_a	Average surface roughness (three dimensional)
S_q	Root mean square (three dimensional)
T	Temperature
T_{Actual}	Actual temperature
T_L	Liquidus temperature
T_S	Solidus temperature
T_m	Melting temperature
T_0	Ambient temperature
t	Time
U	Arc voltage
$\mathbf{u}$	Perpendicular tolerance
$\mathbf{u_m}$	Perpendicular tolerance (mean value)
v	Welding travel speed
W_1 - W_5	Weld width dimensions (in Figure 5.6)
z_b, z_i, z_t	z coordinate parameters of the double-conical heat source

Abbreviations

AAU	Aalborg University
CET	Columnar to Equiaxed Transition
FE	Finite Element
GMA	Gas Metal Arc
HAZ	Heat Affected Zone
LWT	Lindø Welding Technology
MAG	Metal Active Gas
NDE	Non Destructive Evaluation
PMZ	Partially Melted Zone
PWHT	Post Weld Heat Treatment
SAW	Submerged Arc Welding
SM	Single Mode
SMAW	Shielded Metal Arc Welding
S-L	Solid-Liquid
STR	Solidification Temperature Range
TDC	Three Dimensional Conical
3D	Three Dimensional

Thesis Details

Thesis Title:	Hybrid Laser Welding of Large Steel Structures: An Experimental and Numerical Study
PhD Student:	Farhang Farrokhi
Supervisor:	Assoc. Prof. Morten Kristiansen Aalborg University

The main body of this thesis consists of the following peer-reviewed publications:

1 Farhang Farrokhi, Steen E. Nielsen, Rasmus H. Schmidt, Simon S. Pedersen, and Morten Kristiansen, "Effect of Cut Quality on Hybrid Laser Arc Welding of Thick Section Steels," Published in *Physics Procedia*, Vol. 78, pp. 65-73, 2015.

2 Farhang Farrokhi and Morten Kristiansen, "A Practical Approach for Increasing Penetration in Hybrid Laser-Arc Welding of Steel," Published in *Physics Procedia*, Vol. 83, pp. 577-586, 2016.

3 Farhang Farrokhi, Raino M. Larsen, and Morten Kristiansen, "Single-Pass Hybrid Laser Welding of 25 mm Thick Steel," Published in *Physics Procedia*, Vol. 89, pp. 49-57, 2017.

4 Morten Kristiansen, Farhang Farrokhi, Ewa Kristiansen, and Sigurd Villumsen, "Application of Hybrid Laser Arc Welding for the Joining of Large Offshore Steel Foundations," Published in *Physics Procedia*, Vol. 89, pp. 197-204, 2017.

5 Farhang Farrokhi, Benny Endelt, and Morten Kristiansen, "A Numerical Model for Full and Partial Penetration Hybrid Laser Welding of Thick-Section Steels," Submitted to a peer-reviewed journal [under review], 2018.

6 Farhang Farrokhi, Benny Endelt, Rasmus S. Andersen, and Morten Kristiansen, "Temperature Gradients at the Solidification Front of Deep Hybrid Laser Welds," Submitted to a peer-reviewed journal [under review], 2018.

In addition to the main papers, the following publications have also been made during the course of this Ph.D.

7 Farhang Farrokhi, Jukka Siltanen, and Antti Salminen, "Fiber Laser Welding of Direct-Quenched Ultrahigh Strength Steels: Evaluation of Hardness, Tensile Strength, and Toughness Properties at Subzero Temperatures," Published in *Journal of Manufacturing Science and Engineering: Transactions of the ASME*, Vol. 137(6), pp. 061012, 2015.

8 Antti Salminen, Farhang Farrokhi, Anna Unt, and Ilkka Poutiainen, "Effect of Optical Parameters on Fiber Laser Welding of Ultrahigh Strength Steels and Weld Mechanical Properties at Subzero Temperatures," Published in *Journal of Laser Applications*, Vol. 28(2), pp. 022415, 2016.

9 Morten Kristiansen, Sigurd Villumsen, and Farhang Farrokhi, "For Hybrid Laser Svejsning Kan Tildannelsen af Svejsefugens Overflade Væsentligt Øge Svejsehastigheden," Published in *Svejsning*, Vol. 44(3), pp. 10-14, June 2017.

Preface

This thesis is submitted as a collection of papers to the Faculty of Engineering and Science at Aalborg University in partial fulfillment of the requirements for the degree of Doctor of Philosophy. The research presented in this thesis has been carried out within the period from October 2014 to February 2018 at the Department of Materials and Production, at Aalborg University.

The research has been a part of the project *Cost-Effective Mass Production of Universal Foundations for Large Offshore Wind Parks* which was supported by Force Technology, Universal Foundation A/S, LIC Engineering A/S, Aalborg University, Department of Materials and Production and Department of Civil Engineering, and Technical University of Denmark, Department of Wind Energy. In addition, this study was supported in part by the Danish National Advanced Technology Foundation.

Acknowledgements

The work on this thesis has been a long and difficult journey. During the course of this study, I have been fortunate to receive support from so many people, to whom I am greatly thankful. However, I would like to take the chance here to appreciate the help that I received from some of these people who deserve particular thank.

First and foremost, I would like to especially thank my supervisor Associate Professor Morten Kristiansen, who gave me such a valuable opportunity to conduct this research and kindly supported me over the entire course of the work.

I would also like to express my gratitude to Associate Professor Mikael Larsen for his kind support and valuable comments on the metallurgical aspects of my research.

I would like to especially thank Associate Professor Benny Endelt for his invaluable guidance during the numerical modeling part of the study.

In addition, my appreciation extends to Ph.D. Steen Erik Nielsen and his colleagues in Force Technology and LWT who always kindly helped me in carrying out the hybird laser welding experiments and testing the samples.

Moreover, I would like to appreciate Professor Ole Madsen and all my colleagues in the group, especially, Assoc. Prof. Simon Bøgh, Assist. Prof. Dimitris Chrysostomou, Ph.D. Rasmus S. Andersen, Ph.D. Sigurd Villumsen,

Ph.D. Casper Schou, and Ph.D. candidate Michael Hansson for providing such a friendly working environment. It has been a great pleasure to work with you.

Finally, I would like to sincerely thank my parents for their kind and endless support in my entire life. I appreciate their patience during the long periods of time that I was far from them during this Ph.D. work.

Farhang Farrokhi Aalborg University, February 26, 2018

Part I

Introduction

Chapter 1

Introduction

1.1 Background and motivation

Due to the worldwide concern about the environment, the interest in technologies for generating renewable electrical energy, such as wind turbines, has been significantly increased, Morren and de Haan [2005]. In general, both onshore and offshore wind technologies indicate relatively low environmental impacts, especially when compared with other electricity generation options (e.g. coal fired or nuclear power plants), Kaldellis et al. [2016].

Fig. 1.1: Offshore wind foundations, Kristiansen et al. [2017]. (a) Suction bucket jacket. Photo: Courtesy of DONG Energy. (b) Two mono buckets on a jack up vessel for installation. Photo: Courtesy of Universal Foundation.

However, from an economical point of view, the capital price of offshore wind turbines is higher than onshore types. This is partly due to the fact that more infrastructure investments are required and services are more expensive for offshore operations. Moreover, the offshore environment is significantly more uncertain and difficult than onshore, Snyder and Kaiser [2009], leading to more

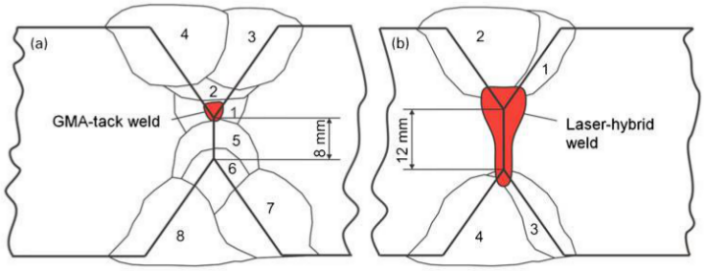

Fig. 1.2: (a) Weld consisting of Gas Metal Arc tack weld and Submerged Arc Welding filler layers; (b) weld consisting of 12 mm deep hybrid laser weld and Submerged Arc Welding filler layers, Gook et al. [2014].

conservative design considerations. For example, offshore foundations require more steel, and therefore, more welding operations for jackets and pilings than the less sophisticated onshore foundations.

One of the ways to reduce the production costs of large steel structures such as offshore wind turbine foundations (Figure 1.1), is to use hybrid laser welding technology. Taking the advantage of this technology makes it possible to reduce the number of welding passes and to minimize the heat distortion compared with that seen in conventional arc welding techniques, [Gook et al., 2014; Reisgen et al., 2012; Webster et al., 2008]. As can be seen in Figure 1.2, welds consisting of for example, a deep hybrid laser weld as the root pass, allow considerably less welding passes, machining, and material consumption compared with welds consisting of only arc welding. Moreover, estimations in shipbuilding industry shows that reworking caused by welding distortions, costs between 20 to 30% of the total man-hours used, which can be reduced significantly by the use of hybrid laser welding, Webster et al. [2008].

Such motivations can be seen in the trends found in heavy industries, where they are looking for new opportunities for substituting their conventional welding methods with hybrid laser welding, Nielsen [2015]. However, in such applications that require thick-section welding, challenges remain yet in developing laser welding techniques to compete with conventional welding methods, Lawrence and Li [2018].

1.1.1 Project description and laser facilities

This study is a part of the *Cost-Effective Mass Production of Universal Foundations for Large Offshore Wind Parks* project. The project was supported by the Danish National Advanced Technology Foundation and the following partners:

- Force Technology.

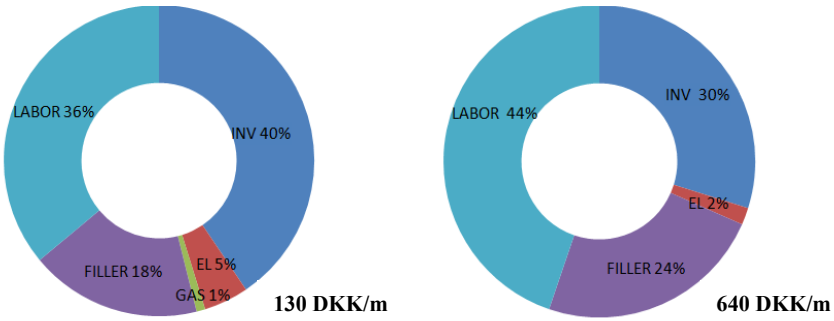

Fig. 1.3: Initial cost analysis for welding of 60 mm thick plates (5-year period): comparison of a combined hybrid laser welding and arc welding procedure with an arc welding only procedure, (adapted from Nielsen [2014b]). DKK/m: Danish Krone per meter; EL: Electricity; INV: Investment; MAG: Metal Active Gas; SAW: Submerged Arc Welding; SMAW: Shielded Metal Arc Welding.

- Universal Foundation A/S.
- LIC Engineering A/S.
- Aalborg University, Department of Materials and Production.
- Aalborg University, Department of Civil Engineering.
- Technical University of Denmark, Department of Wind Energy.

The project aims to develop the design and production of foundations for wind turbines with the consideration of optimization in costs for mass production, Nielsen [2014a]. The project focuses particularly on the bucket foundation designed by Universal Foundation A/S that has been considered for mass production (Figure 1.1, b). The foundation can be easily installed, can be applied and designed for different offshore locations and conditions, and is suitable for industrialization and customization. Installation of such foundations have minimal environmental impact regarding underwater sound emissions. It is also possible to remove the total all-in-one unit by reversing the suction process, and thereby reuse or recycle them, Kristiansen [2014]. Bucket foundations can be potentially the preferable in the market (water depth < 55m), as they significantly reduce the costs of the offshore foundations for the wind farms, Nielsen [2014b]. The initial cost analysis for the manufacturing of these foundations reveals that using hybrid laser welding instead of conventional arc welding, e.g. submerged arc welding (SAW), can potentially reduce the welding costs, and

therefore, the manufacturing costs significantly. This has been depicted in Figure 1.3 where the two processes have been compared in terms of the expenses in a 5-year period.

The main laser facilities available for this project were a 3 kW single mode fiber laser unit at Aalborg University and two disk laser units at Lindø Welding Technology (LWT) each providing a laser with the maximum of 16 kW power. Figures 1.4 and 1.5 show the laser facilities.

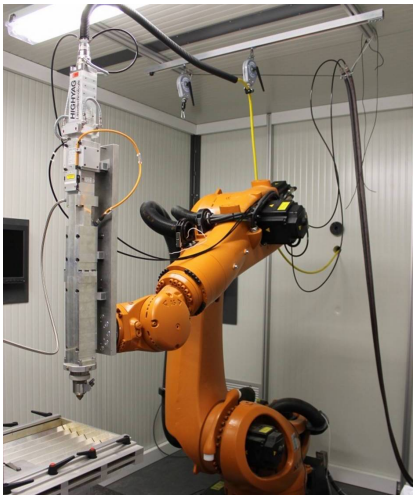

Fig. 1.4: 3 kW single-mode fiber laser unit: Aalborg University, Department of Materials and Production.

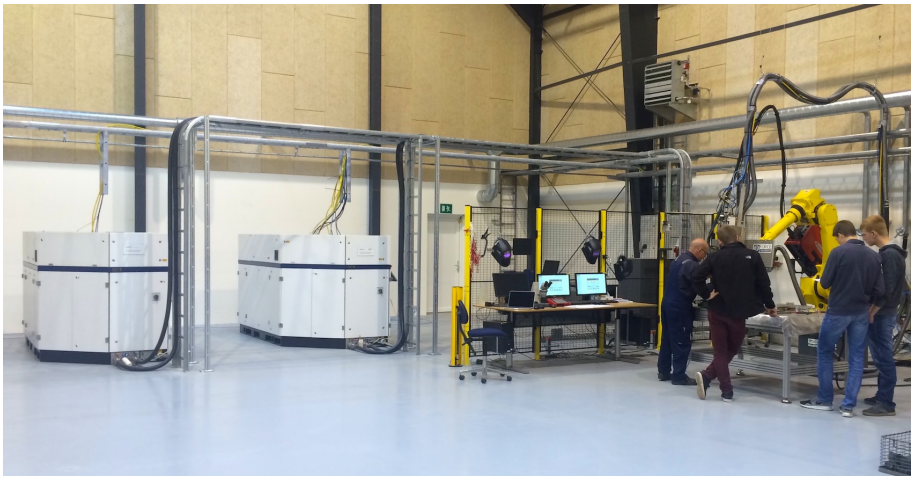

Fig. 1.5: 16 kW+16 kW disk laser unit: LWT.

1.1.2 Initiating problems

According to the initial experiments with the high power laser facilities in LWT, [Hojerslev, 2013; Honore and Hojerslev, 2013], two challenges were predominant when welding thick-section steels: (i) the use of both disk lasers sharing the same melt pool (twin spot) may result in instabilities during the process; (ii) the avoidance of solidification cracking is difficult in the welds. Concerning the first challenge (i), it was suggested to use the laser beams individually e.g. one for the cutting of the plates and generating the grooves, and the other for the subsequent welding. Solving these challenges, however, required further fundamental research and more in-depth knowledge on the subjects. In this regard, an initiating research problem was broadly defined as stated in the following table.

Initiating Problem
How can the dual laser facilities (16 + 16 kW) at LWT be employed for increasing the manufacturing efficiency of bucket foundations?

Later, in Chapter 3 the detailed research objectives of this PhD study will be defined based on the initiating problems. Figure 1.6 depicts the general strategy of the study.

Fig. 1.6: General strategy of the study.

1.2 Scope and limitations

This thesis aimed for carrying out an experimental and numerical investigation in order to address the research questions that are posed in Chapter 3. More specific scope and objectives can be found in each paper separately.

The welding experiments were mainly limited to butt joint configuration. Based on the materials required for the manufacturing of bucket foundations, S355J2 steel plates with a thickness of 25 mm were chosen for this study. This was because one of the main parts of the bucket foundation that is called skirt, mainly consisted of S355J2 plates with different thicknesses of up to 25 mm. However, to allow comparison, in some cases, plates with smaller thicknesses were also included in the research.

The definition of thick-section steels, to some degree, is arbitrary in the

literature. In this study, plates with the thicknesses of 10 mm and above were considered as thick-section. Nevertheless, the attempt was to focus more on the plates having the thickness of 20 mm and above.

It is worth mentioning that the study was strictly limited to the equipment that were available within the PhD project period.

Finally, it should be noted that the subject of numerical modeling was employed as a tool for providing further understanding on the experimental observations. Therefore, the review of the numerical modeling techniques and theories was excluded from the literature review section and remained limited only to the introduction of the corresponding sections and papers in this thesis. Further information on the theories of numerical modeling can be found in the textbooks and the theory manual of LS-DYNA LSTC [2017].

1.3 Experimental and computational equipment

The following equipment have been used during the research as the **main tools**:

- Aalborg University's 3 kW SM fiber laser (Figure 1.4) for the laser cutting experiments.
- Lindø Welding Technology's 2x16 kW disc laser (Figure 1.5) for the hybrid laser welding experiments.
- Force Technology and Aalborg University's laboratories for the preparation and testing of the specimens.
- Aalborg University's Linux computer cluster for Finite Element computations. The computer cluster is a Dell solution with 5 nodes, each containing two Intel Xeon E5-2697v3 (2.6 GHz) processors with 14 cores and 256 GB RAM. Every Finite Element computation in this thesis used 16 processors in parallel.

1.4 Outline of thesis

This PhD thesis has been formulated as a collection-of-papers, meaning that the thesis consists of an introduction and the summary report of the research, followed by the related publications. The thesis contains three parts with six chapters in total. Part I provides an introduction to the thesis. This part begins with Chapter 1, in which the background and motivations of the project, initiating problems, and the general information are presented. Chapter 2 contains the literature review and the main challenges related to the PhD subject and the initiating problems. Finally, based on the background and the review, two research objectives (1 and 2) and research methodologies are presented in Chapter 3.

Part II consists of a summary report presenting the main contributions and the results of this PhD study. This part has been formulated as the summaries of the main included papers (**Papers 1-6**) as well as the complementary information that have not been published in the papers. In this part, Chapters 4 and 5 contain the summary reports in relation to the research objective 1 and 2, respectively. The general conclusion on this thesis and directions for future work is described in Chapter 6.

Part III contains the papers on which the summary reports is based. The overall structure of the thesis can be seen in Figure 1.7.

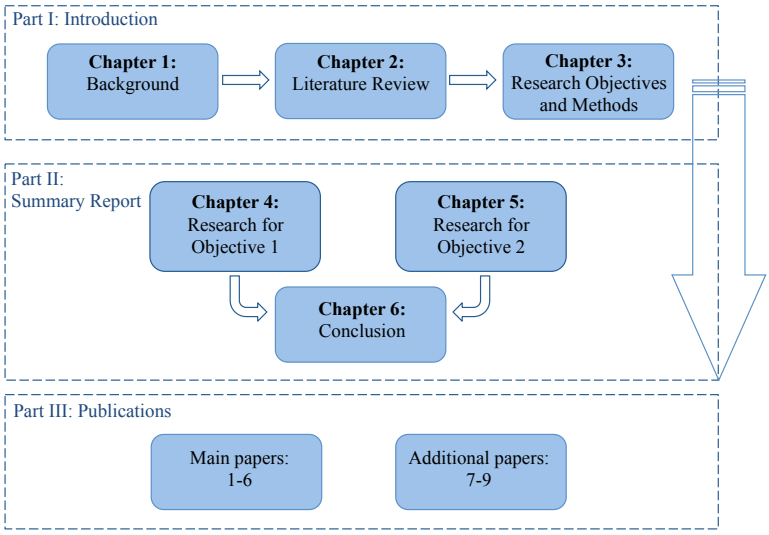

Fig. 1.7: Overall structure of the thesis.

Chapter 2

Literature Review

As the focus of this PhD project is on the laser cutting and welding of thick-section steels, a brief introduction to the relevant subjects is necessary before presenting the research. Accordingly, this chapter starts with introducing laser cutting and hybrid laser welding technologies and then presents a literature review on these processes in relation to the processing of thick section steels. Finally, weld solidification cracking in laser welds will be reviewed as one of the main challenges of thick-section welding. Basic principles of lasers and laser materials processing can be found in Steen and Mazumder [2010], and therefore, are excluded from this chapter.

2.1 Laser cutting of thick-section steels

Laser cutting is a well-established thermal cutting process, which can be used effectively for a wide range of materials. This technology takes the advantages of an intensely focused laser beam to melt and possibly vaporize the workpiece and a pressurized assist gas jet to blow the melt or vaporized layer out of the cut kerf (Figure 2.1). The most applicable laser cutting techniques for metals are fusion cutting and reactive or oxygen-assisted laser cutting which use nitrogen and oxygen assist gas respectively, Dahotre and Harimkar [2008]. For mild and carbon steels the latter is the most common since the oxygen assist gas provides more energy to the cut zone leading to higher processing speeds, and also reduces the viscosity of the melt in the cut zone which minimizes the creation of dross, Pocorni et al. [2013]. In general, for a given laser type, the productivity and the quality of the cut are influenced by several parameters such as laser power, cutting speed, assist gas pressure, assist gas type, and focal point position, Lan et al. [2011].

The main quality challenges of laser cutting of thick-section steels, particularly with oxygen assist gas, can be listed as following:

- Cut edge surface roughness quality (i.e. the striation).
- Dross formation (recast layer) on the lower cut edge.
- Deviation in perpendicularity of the cut edges (kerf size and shape).

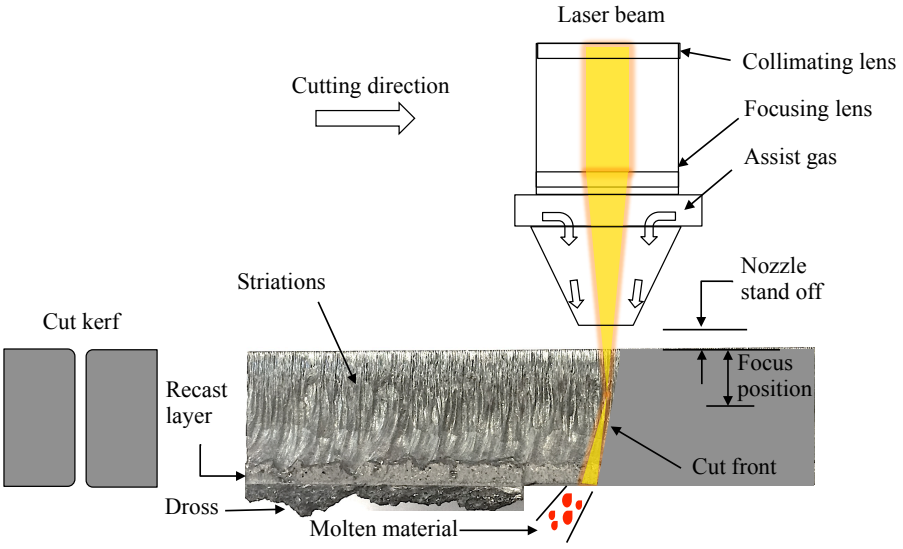

Fig. 2.1: Principles of laser cutting of thick-section steels and the typical quality challenges.

According to Wandera et al. [2011], the formation of striations is attributed to the erosion of the cut edge caused by the exothermic reaction of the oxygen assist gas, which develops the striations on the cut edge when cutting with oxygen assist gas. Regarding the dross formation, studies show that the surface tension of the melt limits the melt-ejection speed, which is followed by building-up of melt at the bottom of the kerf, and therefore, leads to incomplete ejection of the molten material, Tani et al. [2003].

A great deal of research has been conducted to obtain knowledge on the origins of the mentioned challenges in laser cutting of thick-section steels. For example, on the formation of laser cut striations, more information can be found in Goppold et al. [2014]; Orishich et al. [2014]; Pocorni et al. [2014]; Rao and Nath [2002]; Stelzer et al. [2013]; Wandera et al. [2011]; Yilbas [2008]; Yudin et al. [2014]; Zaitsev and Ermolaev [2014]. Similarly, about the dross formation and kerf size variation, further information can be found, for example in Orishich et al. [2014]; Wandera and Kujanpaa [2011]; Wandera et al. [2011]; Yilbas [2008]; Yilbas, B.S., Abdul Aleem [2006]. In general, it can be said that laser cutting is more effective for material thicknesses of less than 20 mm, Lawrence and Li [2018]. This can be mainly attributed to the fact that when the material thickness increases, less laser energy reaches the bottom of the plate and also the gas pressure drops, and hence, material removal efficiency is reduced.

Moreover, the difference between CO_2 and solid-state lasers, in terms of their influence on the cut quality, has been discussed in Ivarson [2017]; Lawrence

and Li [2018]; Mahrle and Beyer [2009]; Orishich et al. [2014]; Petring et al. [2012]; Pocorni et al. [2014]; Poprawe et al. [2010]; Scintilla et al. [2011]; Yudin et al. [2014]. Compared to CO_2 lasers, solid-state lasers (fiber/disk) have higher energy efficiency (electrical to optical conversion), and also thanks to their shorter wavelength, they benefit from the higher absorptivity for metallic materials. However, in laser cutting, these advantages seem to be more beneficial when the thicknesses are below 5 mm. Above this thickness, CO_2 lasers have exhibited higher cut qualities, Lawrence and Li [2018]. Although, much research is yet required on this subject, so far, this difference in quality may be mainly attributed to the different incident beam angle caused by the cutting front geometry that seems to be dependent on the lasers wavelength, Mahrle and Beyer [2009].

In general, central to all of these studies, it can be said that obtaining high quality cuts in laser cutting of thick-section steels is considerably more challenging compared with the laser cutting of thin sheets. Surprisingly, the challenge is more pronounced when using solid-state lasers, even though attention to the solid-state lasers is growing in industry.

2.2 Hybrid laser welding of thick-section steels

Hybrid laser welding is a promising welding process that is suitable for processing thick-section steels. This is due to the general fact that it compensates for the limitations in laser welding and arc welding by utilizing the features of both. Comparing with laser welding and arc welding as individual processes, hybrid laser welding has many advantages such as deeper penetration, higher welding speeds, wider gap tolerance, better weld bead surface appearance and reduced welding defects, Katayama [2009]. Figure 2.2 illustrates the principles of hybrid laser welding, in which the arc system is Gas Metal Arc (GMA) and the welding configuration is laser leading.

Hybrid laser welding of structural materials has been the subject of intensive research and development for almost three decades. The challenges which have been investigated may be grouped into equipment, process, quality, monitoring, non-destructive evaluation (NDE) and materials-related issues, Kristensen [2009]. In this section, the focus will be on the main weld quality challenges. Hybrid laser welding, as a fusion welding process, is subjected to many different weld imperfections and defects. Characteristics of these quality issues can be found in the literature e.g. Olsen [2009]; Victor [2011]. Most of the weld quality issues can be controlled by the welding process parameters. However, as the thickness of the steel increases, pores and solidification cracks are more prone to occur, Kristensen [2009]. The latter is more critical due to their flat and sharp geometrical character.

With the development of high power laser systems over the past decade,

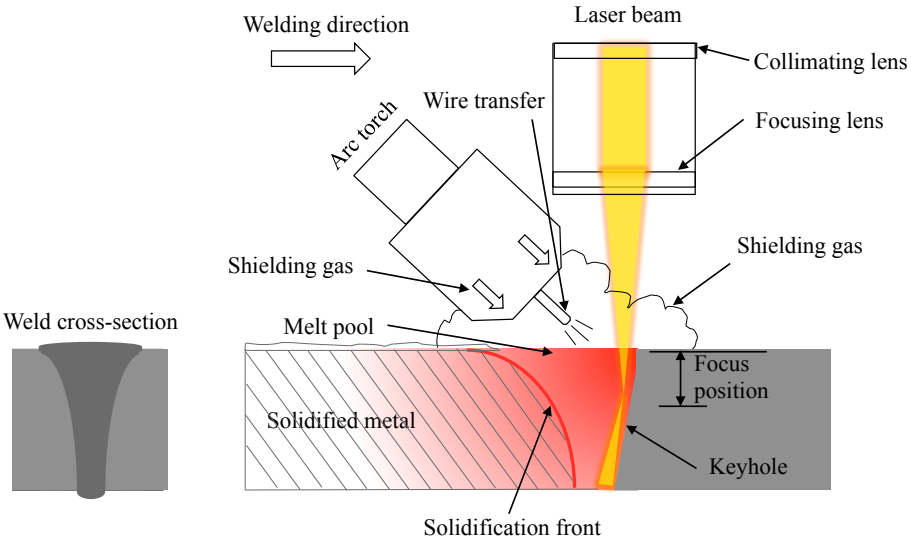

Fig. 2.2: Principles of hybrid laser welding of thick-section steels.

a great deal of research has been conducted on the hybrid laser welding of thick-section steels. Among these works, several experimental studies have attempted to obtain crack-free welds of steel plates having wall thicknesses exceeding 20 mm, [Akselsen et al., 2013; Chen et al., 2013; Gook et al., 2014; Hojerslev, 2013; Nielsen, 2015; Rethmeier et al., 2009; Vollertsen et al., 2010; Wahba et al., 2016; Webster et al., 2008].

According to the aforementioned studies, it can be said that the occurrence of solidification cracking in laser welds of thick-section steels seems to be too complicated to be simply controlled by the process parameters. In addition to the choice of process parameters and filler materials, it is evident that joint preparation has a key role in obtaining quality welds. However, due to the complexity of the subject, a universally accepted rule or guideline for avoidance of such defects has not been developed yet and more investigations are required. This subject will be explained more thoroughly in the next section.

Following the importance of the joint preparation, it is important mentioning that the vast majority of the experimental studies in the literature has used milling as preparation technique. However, the influence of laser cutting as a preparation technique on the subsequent hybrid laser welding has not been investigated properly. Studies show that absorptivity of solid-state lasers can be strongly modulated by the roughness level of steel surfaces, [Bergström et al., 2007; Kaplan, 2012b]. This has also been anticipated in practice of laser welding of steels, Sokolov et al. [2015, 2012], where an optimum surface roughness range resulted in higher laser penetration due to the increased laser energy

absorption, Sokolov et al. [2012]. However, considering the lack of sufficient investigation on this subject, it is of great importance to study the influence of laser cut characteristics such as, striations roughness and kerf shape on the subsequent hybrid laser welding process.

2.3 Solidification cracking in laser welds

One of the crucial defects that can occur during welding is cracking, Kou [2015]. Due to their geometrical characteristics, the presence of cracks in the welds can act as stress raisers in the joint and consequently lead to failure and catastrophic results. According to ISO 13919-1 and ISO 12932 standards, solidification cracks are classified as severe defects, which are not tolerated in the welds. Therefore, understanding of the origins of these defects is of great importance for every fabrication process that involves welding. In this section, first the crack types are presented in brief, then the theories and influencing factors of solidification cracking will be explained in general, and finally the subject will be reviewed with a special attention to the hybrid laser welding of thick-section steels.

In welding, fabrication-related cracks can be broadly categorized by the temperature in which they occur. Table 2.1 summarizes these cracks in the three categories of cold cracks, warm cracks, and hot cracks according to Lippold [2015]. It should be noted that these types of cracks are different than the service-related cracks, namely fatigue cracks and corrosion cracks, that may occur after the fabrication. As Lippold [2015] explains:

Cold cracking occurs at or near room temperature and is often referred to as hydrogen induced cracking. This type of cracking can be either intergranular or transgranular and often appears in the Heat Affected Zone (HAZ).

Warm cracking occurs at elevated temperatures yet in the solid state. These forms of cracking are associated with grain boundaries and may appear in both the fusion zone and HAZ. It is important to notice that these cracks are some times referred as ”hot cracks” due to the unclear and arbitrary definition of these terms.

Hot cracking is associated with the presence of liquid in the microstructure, and thus occurs above the solidus temperature. Hot cracking may appear in fusion zone and Partially Melted Zone (PMZ) of HAZ and is usually related to the liquid films along grain boundaries, Lippold [2015]. As was mentioned, this report is mainly focused on weld solidification cracking (see Figure 2.3) which is under the category of hot cracks according to Table 2.1.

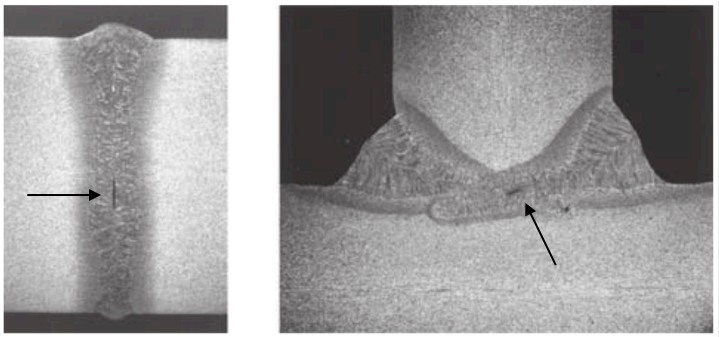

Fig. 2.3: Solidification cracks indicated in hybrid laser welded structural steels: (a) an I-joint 15 mm butt weld and (b) a T-joint in 12 mm plate thickness, Kristensen [2009].

Table 2.1: Fabrication-related cracks according to Lippold [2015]. PWHT: Post Weld Heat Treatment.

Cold cracks	Warm cracks	Hot cracks
Hydrogen induced crack	Ductility dip	Weld solidification crack
Delayed crack	Reheat/PWHT	HAZ liquation
	Strain age	Weld metal liquation
	Liquid metal embrittlement	

2.3.1 General theories and influencing factors

Despite the fact that weld solidification cracking has been the subject of great deal of research over the past decades, the origins of this phenomenon has not been clearly understood yet, [Coniglio and Cross, 2013; Cross, 2005; Lippold, 2015]. Generally it can be said that, solidification cracking appears on the weld centerline and occurs in the final stage of solidification, when a liquid film may appear along the solidification boundaries. It is, in fact, the inability of this liquid film to deal with shrinkage-induced strain and extrinsic mechanical strain during solidification and subsequent cooling of the weld that results in the formation of a solidification crack, Lippold [2015].

Several theories have been proposed over the past 70 years in order to explain the origins of hot cracking in the welds. The most pronounced ones are *Shrinkage-Brittleness theory* by Bochvar and Sviderskaya [1947]; Medovar [1954]; Pumphrey and Jennings [1948]; Toropov [1957], *Strain theory* by Apblett and Pellini [1954]; Pellini [1952], *Generalized theory* by Borland [1960], *Modified generalized theory* by Matsuda [1990]; Matsuda et al. [1982], *Technological strength theory* by Prokhorov and Prokhorov [1971], *Critical stress theory* by Zacharia [1994]; Zacharia and Aramayo [1993], *Rappaz-Drezet-Gremaud*

(RDG) theory by Rappaz et al. [1999], and very recently a new criterion that was proposed by Kou [2015].

The cause of these cracks can ultimately be attributed to the complex interaction between the influences of three factors: (i) welding parameters (thermal cycles), (ii) the chemical composition of the alloy (metallurgy), and (iii) restraint intensity (design), Cross [2005]. These factors however, can be classified in several different ways, depending on the point of view and the purpose of the study. In this report, the influencing factors are described as (i) metallurgy, (ii) thermally induced strains, and (iii) mechanically induced strains.

Metallurgy

From the metallurgical point of view, chemical composition has a dominant effect on weld solidification behavior and therefore, it is of great importance to know the role of elements in the solidification cracking. However, predicting cracking susceptibility based on binary phase relationships usually is not recommended and it is important to consider all the elements present when investigating the weld solidification cracking susceptibility.This is possible by either using modern computational tools e.g. Thermocalc, or employing empirical relationships that are available in the literature, Lippold [2015].

According to Kou [2003], the chemical composition of the weld metal can directly or indirectly affect the following metallurgical factors that have been known to influence the solidification cracking susceptibility. Some of them will be explained briefly in the following text.

- The solidification temperature range (STR).
- The amount and distribution of liquid at the final stage of solidification.
- The ductility of liquid film.
- The primary solidification phase.
- The surface tension of the grain boundary liquid.
- The grain structure.

Solidification temperature range (STR). Solidification temperature range has a key role in solidification cracking susceptibility. Its value can be defined as the difference between liquidus and solidus temperatures. For non-equilibrium solidification, however, it is the lowest melting eutectic in the system that defines the solidus temperature, Cross [2005]. Generally, the wider the solidification temperature range, the larger the mushy zone and thus the larger the area that is weak and susceptible to solidification cracking. Impurities such as S and P are known to have significant influence on promoting solidification cracking in carbon steels. This is due to their strong tendency to segregate at grain boundaries, Hondros and Seah [1977], and form low-melting-point compounds (e.g. Fe-S) that promotes widening the solidification

temperature range, Kou [2003].

The ductility of liquid film. Generally speaking, the less ductile a solidifying weld metal is, the more likely it will crack during solidification. The addition of carbon content in carbon steels reduces the ductility of liquid film, Lancaster [1999]. This is due to the tendency of carbon to promote austenite (fcc) solidification mode. At these high carbon levels the segregation effect of P and S are more pronounced during austenite solidification, Lippold [2015].

The primary solidification phase. The primary solidification phase can affect the solidification cracking susceptibility of carbon steels. Harmful impurities such as S and P are more soluble in delta-ferrite than in austenite. According to Fe-C phase diagram, when the carbon content is greater than 0.53, austenite becomes the primary solidification phase and solidification cracking becomes more likely Kou [2003]. However, in the case of low carbon steels, the primary solidification phase is often as ferrite (bbc crystal structure) which will improve the cracking resistance in the welds, Lippold [2015].

The grain structure. It has been generally accepted that coarse columnar grains are more susceptible to cracking than fine equiaxed grains. This is due to three facts: (i) fine equiaxed-grained structure can deform to accommodate contraction strains more easily, which means, it is more ductile, than columnar-grained structure; (ii) liquid feeding and healing of initiate cracks can be more effective in fine-grained material; (iii) the grain boundary area is much larger in fine-grained material and, therefore, harmful low-melting-point segregates are less concentrated at the grain boundary, Kou [2003]. Concerning the latter, it can also be said that when the grain boundary area is larger, a smaller amount of strain is partitioned to each individual grain boundary, Cross [2005].

So far, the metallurgical factors that were discussed were mainly influenced by the chemical composition and alloying elements. However, the grain structure, in addition to the chemical composition, is also very dependent on the welding process parameters. In general, high travel speeds result in elongated "teardrop"-shaped weld pools with columnar grains growing normal to the welding direction that are generally susceptible to centerline cracking. It is usually recommended to either reduce the weld travel speed, or to use alternative techniques for grain refinement in the weld. The subject of grain refinement has been extensively studied in welding of aluminum alloys, [Arata et al., 1974; Ganaha et al., 1980; Garland, 1974; Kou and Le, 1988; Norman et al., 1998; Pearce and Kerr, 1981; Schempp et al., 2014a,b], stainless steels, [Kurz et al., 2001; Reddy and Mohandas, 2001; Villafuerte and Kerr, 1990; Villafuerte et al., 1995, 1990], and ultra high strength steels, Mohandas et al. [1997].

The attempt in all of these studies was to promote columnar to equiaxed transition (CET) in the weld. According to these studies, CET can be obtained

by the combination of the following factors:

- The optimization of process parameters and solidification parameters namely, solidification growth rate and temperature gradients of the liquid;
- The addition of nucleant particles (e.g. TiB_2 in aluminum alloys) that promote heterogeneous nucleation;
- Alternative methods e.g. vibration or magnetic stirring during welding.

It is very important to notice that in contrast to the effect of travel speed alone, when the coupled effect of speed and power is considered, then a high travel speed may result in a beneficial grain structure. Sufficiently high welding travel speed and power may promote grain refinement that is in the favor of cracking resistance. This can be explained by the solidification mechanisms in welding. In metal alloys, solidification mode is influenced by the combination of the temperature gradient of the liquid, G_L, and solidification growth rate, R, Lippold [2015].

$$G_L = \frac{dT_L}{dx} \tag{2.1}$$

$$R = \frac{dx}{dt} \tag{2.2}$$

where T is the temperature and t is the time. The vector product of temperature gradient, G, and solidification rate can represent the local cooling rate at the solid-liquid interface.

$$G \cdot R = \frac{dT}{dx} \cdot \frac{dx}{dt} = \frac{dT}{dt} \tag{2.3}$$

Figure 2.4 schematically shows the effect of these factors on solidification modes. Normally, equiaxed dendritic growth is very seldom in welding due to the large constitutional supercooling required, Rutter and Chalmers [1953]. However, as shown in Figure 2.4, if the temperature gradient is extremely low, equiaxed dendritic growth can be possible at high solidification rates (high travel speeds). This has also been experimentally observed by many studies, for example in Arata et al. [1974]; Ganaha et al. [1980]; Kou and Le [1988] higher heat inputs and welding speeds promoted the formation of equaixed grains in welding of commercial aluminum alloys. However, the authors, observed that the presence of some compounds in the liquid promoted the equiaxed nucleation. As Kou [2003] explains, consequently, it was concluded that (i) heterogeneous nucleation aided by (ii) constitutional supercooling result in the formation of equiaxed grains in the fusion zone. Figure 2.5 schematically illustrates the coupled influence of welding speed and heat input on the solidification mode. Moreover, other alternative techniques can also be used for grain refinement. For example, pulsing the welding current or weaving the bead from side

to side, Lippold [2015], vibration, Garland [1974], and magnetic stirring, Pearce and Kerr [1981] have been extensively reported on aluminum alloys.

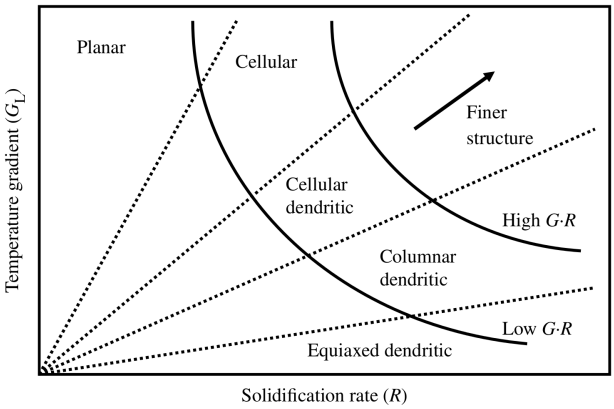

Fig. 2.4: Effect of temperature gradient in the liquid, G_L, and solidification growth rate, R, on solidification mode (From Lippold [2015]).

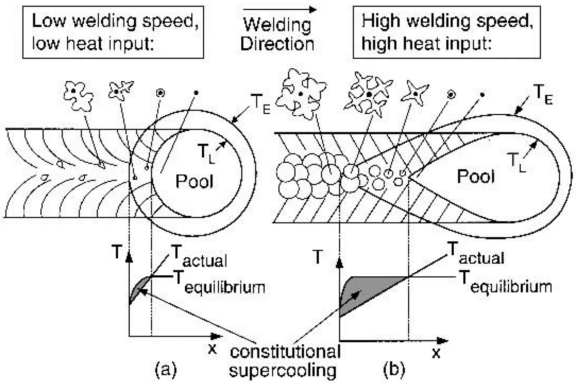

Fig. 2.5: Effect of welding parameters on heterogeneous nucleation: (a) low constitutional supercooling at low welding speed and heat input; (b) heterogeneous nucleation aided by high constitutional supercooling at high welding speed and heat input, (From Kou [2003]).

Thermally-induced strains

According to Lippold [2015], two fundamental conditions must be satisfied for weld solidification cracking to occur: (i) a crack-susceptible microstructure (metallurgy), which was discussed in the previous section, and (ii) thermally and/or mechanically imposed strains, which will be presented in the following

sections. In general, thermally-induced strains are primarily controlled by the welding process parameters and heat treatments.

Process parameters. During solidification, the weld undergoes a volumetric shrinkage due to the liquid-solid phase change, which is in the range from 3 to 8% for metallic systems, Lippold [2015]. In addition to the solidification shrinkage, during cooling, the weld is also restrained by an un-even thermal contraction of the surrounding solid material. The main process parameters of welding govern both of these strain mechanisms, and thereby the chance of solidification cracking. As a general rule of thumb, the less heat imposed into the material, the less the thermally induced strains will be. This is why the use of high-intensity heat sources such as electron or laser beams significantly reduces the distortion of the workpiece, Kou [2003]. However, when hot cracking is the subject, it is very important to pay special attention to the local strains in melt pool and mushy zone. For example, according to the results of 3D multi-scale simulation of welding in Zareie Rajani and Phillion [2016], increasing the welding travel speed increases the internal deformation rate of the weld mushy zone. This shows the role of complex thermo-mechanical factors involved and the complexity of solidification cracking phenomenon.

Heat treatment. Any heat treatment process that changes the temperature gradients in the workpiece, can also influence the chance of cracking. For example, it has been suggested extensively by numerous studies that preheating the workpiece reduces strains, Kou [2003]. However, it should be noted that pre-heating is not so cost-efficient and practical, particularly when it comes to thick-section welding and manufacturing of large structures.

Mechanically-induced strains

Apart from the thermally-induced strains discussed in the welding process parameters section, welds can also be restrained mechanically. The origin of this type of restraint can be attributed to the following factors:

- The design features such as joint geometry before and after the welding.
- The degree of restraint of the workpiece that is derived by the strength, density, and dimensions of the workpiece.
- The mechanical fixturing and pre-load.

Joint geometry. Joint geometry before welding includes the preparation and design of groove geometry that often indirectly influence the chance of solidification cracking. In fact, it is the groove shape or area that determines how many passes with what sequences, and how much heat input are required for the welding. The thermo-mechanical response of the worpiece varies depending on whether V groove, X groove, or double Y groove has been used for the same

material and thickness. Another important aspect of this subject is the weld sequences, when more than one pass is required. For example, level of restraint is significantly higher during the second pass (side) of a double-sided joint, Kou [2003]. The effect of joint design can be particularly more pronounced in the case of high-energy intensity (e.g. laser) welding of thick-section plates. However, despite the importance of the subject there are not enough studies available on this subject, which will be discussed in Section 2.3.2.

Joint geometry after the welding includes the geometrical characteristics of the weld such as weld bead shape and dimensions. These characteristics can be mainly controlled by welding process parameters as well as the groove design that was discussed earlier. Weld bead shape can influence the level of restraint that builds up in the weld during the final stages of solidification. In general, the tensile stresses along the outer surface of concave welds are larger compared with that of convex welds. Therefore, concave welds are more prone to the centerline cracking that initiate from the outer surface. In addition to the weld bead shape, the depth/width ratio can also influence restraint within the weld during solidification, and thereby solidification cracking. However, as will be discussed later, avoiding such situations can be difficult in high energy intensity welding processes, such as laser welding and electron beam welding, due to their inherent nature, [Kou, 2003; Lippold, 2015].

The degree of restraint of the workpiece. Every welding workpiece has some inherent characteristics that are often not an option to change. These characteristics that can potentially increase the level of restraint include material's strength, density, geometry, and dimensions. The combination of these factors is also known as the degree of restraint of the workpiece, Kou [2003]. The strength level of the base metal can affect the restraint in the HAZ during solidification. For example, when welding precipitation-strengthened materials, such as Ni-base superalloys, lower-strength filler metals can be used to reduce the shrinkage stress, Lippold [2015]. Similarly, the dimensions and thickness of the workpiece has an important role in influencing the level of restraint. Generally speaking, large structures and thick-section plates increase the level of restraint. In such cases, locating welds in low-restraint areas may help. However, the role of restraint in the solidification cracking susceptibility, has been controversially discussed, which will be described further in the following paragraph.

Mechanical fixturing and pre-load. During welding, the joint gap tends to vary and also the workpiece may get un-evenly deformed due to the heat input of the process. Therefore, mechanical fixturing is often necessary to maintain the shape of the joint during welding and to avoid quality issues. However, this may be at the cost of increased restraint in the joint. As was mentioned, the influence of restraint has been controversially discussed in the

literature. The general belief is that the higher the level of restraint, the higher is the cracking susceptibility. This is particularly correct in the case of cold cracking that is caused by global residual stresses that increase with restraint intensity. However, in a study of restraint influence on butt joint welding of aluminum plates, Cross and Böllinghaus [2006], it turned out that high levels of restraint intensity and pre-load appear to prevent solidification crack initiation and growth. This is explained by the fact that, in contrast to the cold cracking, solidification cracking is caused by local strains, which are not linked in any simple manner to restraint, Cross and Böllinghaus [2006]. The results of Cross and Böllinghaus [2006]'s study were later confirmed by Kannengiesser and Kromm [2007], using pressure springs that imposed a constant transverse stress on the plate during welding. It can be concluded that compressive forces (or reduced tensile restraint) improve the solidification cracking resistance. Therefore, using fixturing to apply transverse compressive forces may be helpful in some cases.

Summary

According to the influencing factors that were discussed in this section, an overall overview of the subject can be summarized in Figure 2.6.

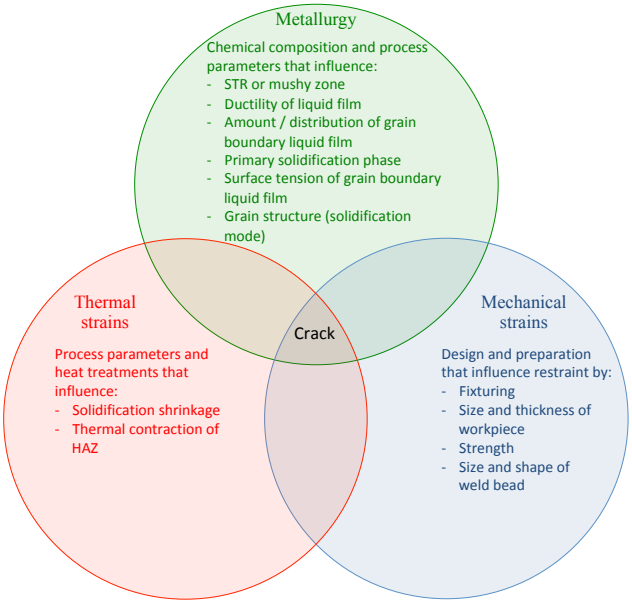

Fig. 2.6: Influencing factors of weld solidification cracking.

2.3.2 Challenges in laser welds of thick-section steels

Based on the influencing factors of solidification cracking and also the experimental investigations in the literature review, it is evident that avoiding solidification cracks in hybrid laser welding of thick-section steels is of great challenge. In such cases, as shown in Figure 2.7, solidification cracks often appear in one of the two susceptible spots of the laser dominated region. Figure 2.7b-d shows hybrid laser welds, in which the crack appeared in about mid-section and root-section of the laser dominated region. The reason of such cracks can be mainly attributed to the high intensity laser heat source that inherently results in a disadvantageous (i) geometry, (ii) microstructure, and (iii) restraint in the weld. The combination of these factors results in the increased risk of solidification cracking in the hybrid laser welding of thick-section steels. The following points will briefly describe these factors.

- **Geometry**. In continuous casting, that in many respects has much in common with welding, Porter et al. [2009], a continuous melt flow is fed downwards to the mold in order to compensate for the voids induced by solidification shrinkage in the center. Similarly, in the case of shallow arc welds, the solidification shrinkage in the depth of the melt pool may be compensated (healed) by the liquid flow from the surface. Whereas, in the case of deep laser welds, the last layer of liquid melt in the depth of the laser dominated region, is way separated from the liquid metal on the upper layers of the melt pool. Therefore, the chance of healing for the solidification shrinkage may potentially be reduced in the laser dominated region.

- **Microstructure**. The typical microstructure that is formed in the laser dominated region consists of steep angled columnar grains that grow from opposite sides of the weld (see Figure 2.7). As was mentioned before, such solidification mode is detrimental for solidification cracking resistance as they tend to form a continuous liquid film by allowing harmful low-melting-point segregates to concentrate at the grain boundary, Kou [2003].

- **Restraint**. Recent studies on the stress fields during the solidification of laser welds (e.g. 10 ms after the heat source passes by), Gebhardt et al. [2013], show that the amount of transverse tensile stresses considerably increases in the two crack susceptible regions of laser welds. As shown in Figure 2.8b two peak values of stress appear in mid-section (evaluation point 1) and root-section (evaluation point 2) of the partial penetration laser welds, which were in agreement with their experimental observations, [Gebhardt et al., 2013, 2014].

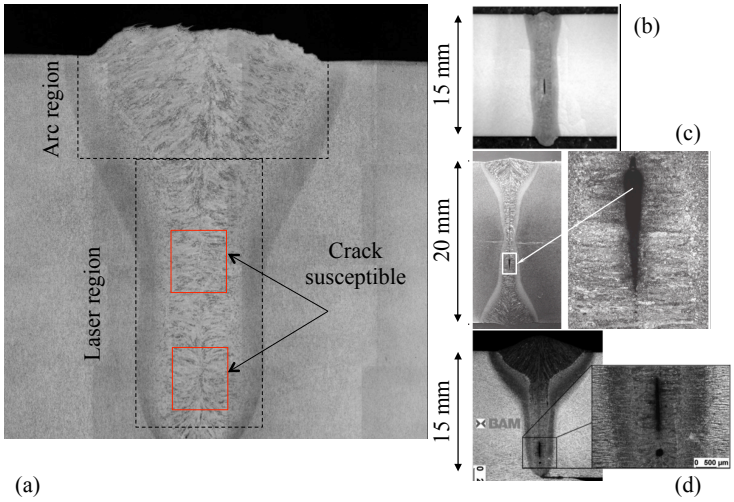

Fig. 2.7: (a) An example of a hybrid laser weld cross-section with 16 mm penetration, Kristiansen et al. [2017], (b-d) solidification cracks in the susceptible regions, (b): HYBLAS [2003], (c): Akselsen et al. [2013], (d): Gebhardt et al. [2014].

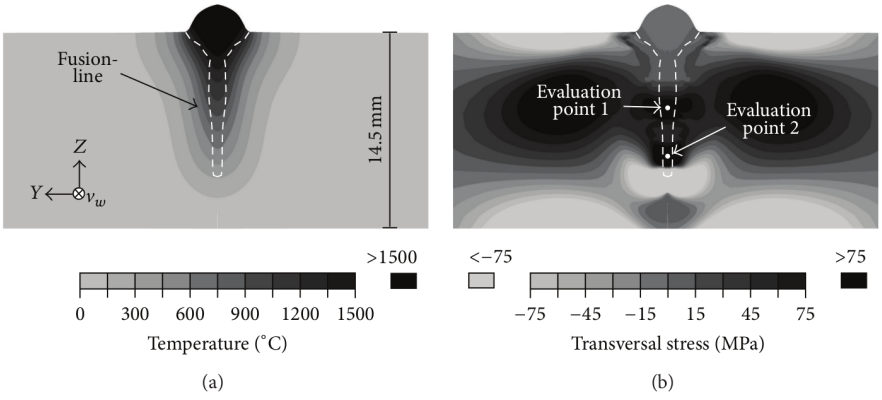

Fig. 2.8: (a) Temperature and (b) transverse stresses in the computational model 10 ms after the laser beam center passed the computational domain, Gebhardt et al. [2013].

As was mentioned previously, several experimental studies have attempted to find solutions for crack-free welding of steel plates having wall thicknesses exceeding 20 mm. According to [Rethmeier et al., 2009; Vollertsen et al., 2010] preheating is helpful for obtaining sound welds in I-joint configuration. Unfortunately, preheating is not so practical for welding of thick-section steels of large structures.

Alternatively, Gook et al. [2014]; Nielsen [2015]; Rethmeier et al. [2009];

Vollertsen et al. [2010]; Webster et al. [2008] suggested using beveled groove (e.g. Y-joint) for obtaining crack-free welds, which shows the importance of edge preparation in this subject. The general belief is that using beveled grooves increases the penetration of filler wire into the groove and thereby allowing the filler material to mix with the base material to assure a proper solidification, Nielsen [2015]. This could also potentially provide the possibility of crack healing by supplying more filler material melt flow further down in the laser dominated region. However, Gook et al. [2014]; Nielsen [2015]; Tsukamoto et al. [2008] showed that the penetration of filler material is limited to certain depths. For example, Gook et al. [2014] measured the distribution of nickel (deposited by the filler material) in hybrid laser welds of X80 pipe steel plates having Y groove geometry. They concluded that no filler material penetration could be detected beyond 14 mm depth limit, and therefore, any metallurgical influence or enhancement on the weld metal properties through the welding wire was not possible beyond this depth. They also observed that the arc type does not have any effect on the dilution character in the laser-dominated region of the hybrid welds.

Wahba et al. [2016] developed a new single-pass hybrid laser welding technique on 25 mm SM490A low-alloyed steel. They used a 2.5 mm gap in butt joint configuration, filled up with cut wires and supported by backing. Using such technique they could obtain sound joints having equiaxed grains in the laser dominated region. However, similar to submerged arc welding, this technique is limited in positional welding as the cut wires need to be fed into the groove in flat position. Although Wahba et al. [2016] presented the welding procedure thoroughly, they did not provide any explanation on the mechanisms of prevention of cracks in their experiments.

Chen et al. [2013] used a horizontal double-sided hybrid laser welding technique (back welding), in which the root was welded by another hybrid laser welding processes simultaneously. Using such technique, they claimed that crack-free welds could be obtained on 30 mm thick high-strength steel joints having K-joint configuration. However, this technique requires two laser units to work in a relatively risky position and share the same melt pool from the opposite sides.

Gebhardt et al. [2012] conducted an experimental study on the full and partial penetration hybrid laser welding of a number of different carbon steels with wall thicknesses up to about 15 mm. They reported that crack-free welds were obtained only when full penetration welding was carried out and shrinkage restraint was limited. Schaefer et al. [2015] analyzed the influence of laser beam quality and parameters on the formation of solidification cracks in tempered steels. Similar to Gebhardt et al. [2012], they also observed that crack formation could be avoided when full penetration of the sample thickness was achieved, while partial penetration experiments required cautious optimization of beam parameters to avoid solidification cracks.

This was explained by a numerical analysis carried out on S460NH low-alloyed high strength steel in Gebhardt et al. [2013]. The results showed that higher magnitude of stresses occurred in the partial penetration-mode and in the regions that solidification cracks were found in the experiments. In a recent study on the hot cracking during laser welding of steel by Schaefer et al. [2017], another explanation was proposed for this phenomenon. Schaefer et al. [2017] related the formation of cracks to melt flow dynamics, which, according to their previous study in Schaefer et al. [2015], differs in full and partial penetration laser welding.

The importance of penetration-mode can be noticed with a closer look at the experimental observations in the literature. Among the studies that suggested crack-free welding procedures for thick-section steels, the vast majority of them used hybrid laser welding only for one pass where full penetration of the sample thickness was achieved and where there was no solid material below the bottom of the laser weld, [Chen et al., 2013; Gebhardt et al., 2012; Gook et al., 2014; Rethmeier et al., 2009; Vollertsen et al., 2010; Wahba et al., 2016; Webster et al., 2008]. Nonetheless, despite the importance of the subject, only a limited number of studies have related the effect of penetration-mode and the design of weld sequences to the chance of cracking and more systematic investigations are required.

2.4 In brief

- Obtaining high quality cuts in laser cutting of thick-section steels is considerably more challenging compared with the laser cutting of thin sheets. Notably, the challenge appears to be more pronounced when using solid-state lasers.
- The influence of laser cutting as a preparation technique on the subsequent hybrid laser welding has not been investigated properly.
- Avoiding solidification cracks in hybrid laser welding of thick-section steels is of great challenge. This is due to the inherent characteristics of the keyhole laser welding process.
- Despite the importance of the subject, only a limited number of studies have related the effect of penetration-mode and the design of weld sequences to the risk of cracking and more systematic investigations are required.

Chapter 3

Research Objectives and Methods

3.1 Objectives

According to the literature review and the initiating problems during the preliminary experiments of the project (stated in Section 1.1.2), two research objectives were determined for this study as follows.

Research Objective 1

In an integrated laser cutting-welding system: what is the influence of laser cut surface characteristics, such as (i) surface roughness and (ii) cut kerf shape, on the quality and efficiency of the subsequent hybrid laser welding?

The specific objectives related to the research objective 1 are listed as following:

- What is the influence of the cut surface roughness (from laser cutting) on the quality and efficiency of the subsequent hybrid laser welding?
- What is the influence of the cut kerf (from laser cutting) on the quality and efficiency of the subsequent hybrid laser welding?
- From an industrial point of view, can the laser cutting be adapted as the joint preparation method for the subsequent hybrid laser welding? If yes, what are the quality and efficiency advantages?

Research objective 1 will be addressed in Chapter 4.

Research Objective 2

How is it possible to reduce the risk of solidification cracking in hybrid laser welding of thick-section steels?

The specific objectives related to the research objective 2 are listed as following:

- Is it experimentally possible to obtain crack-free welds?
- Using the FE method, based only on thermal conduction, is it possible to model full and partial penetration hybrid laser welding and explain the solidification cracking phenomenon?
- What is the influence of penetration-mode on the solidification cracking phenomenon?

Research objective 2 will be addressed in Chapter 5.

3.2 Methodology

The following **key methods** will be used to reach the research objectives:

- Empirical study on laser cutting and hybrid laser welding. This will also include the macro and micro-scale testing of cut and welded samples for evaluating their quality and properties.
- Analytical thermal modeling of hybrid laser welding using numerical methods in order to simulate the process and explain the phenomena observed experimentally.

Part II

Summary Report

Chapter 4

Laser cutting-welding integration

In this chapter, the summary of experiments that have been performed to answer the research objective 1 questions will be presented. First, the general concept of the laser cutting-welding integration system will be introduced. Following the general concept, two laser cut qualities obtained by nitrogen and oxygen assisted gas laser cutting will be presented. Then, the influences of cut surface roughness and groove shape will be discussed separately. Finally, the general conclusions will be presented in the last section. The chapter will be based on the summary of the works presented in **Papers 1-4**.

4.1 General concept

The general concept and the strategy of the integrated laser cutting-welding study has been illustrated in Figure 4.1. The idea is to adapt the laser cutting to the subsequent hybrid laser welding process. In the mass production of large steel structures, for example, the two laser units in LWT can be potentially used for this purpose. In such system, first the laser unit 1 cuts the plates according to the welding requirements, then the laser unit 2 carries out the subsequent welding process according to the preparation strategy. However, due to the limitations of the PhD project, the Aalborg University laser cell, shown in Figure 1.4, was used as the laser unit 1 for the cutting. The welding part was performed in LWT using one of their lasers as the laser unit 2 (Figure 1.5).

4.2 Characteristics of laser cuts

In this research, two types of laser cuts were studied. One cutting used nitrogen as assist gas, and the other used oxygen. As was mentioned before, both types of cutting processes were performed using the 3 kW single-mode fiber laser system in AAU. More information about the laser setup can be found in Kristiansen et al. [2013]. In the following text the characteristics of each cut will be presented.

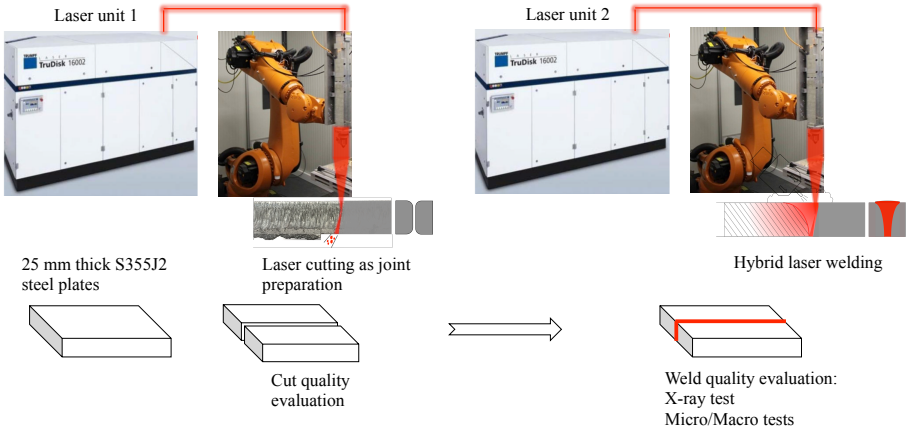

Fig. 4.1: General concept and the strategy of the integrated laser cutting-welding study.

4.2.1 Nitrogen assisted laser cutting

A thorough explanation of the quality characteristics of nitrogen assisted laser cuts and the corresponding cutting procedure has been presented in **Paper 1**: *Effect of Cut Quality on Hybrid Laser Arc Welding of Thick Section Steels*, Farrokhi et al. [2015a] and **Paper 2**: *A Practical Approach for Increasing Penetration in Hybrid Laser-Arc Welding of Steel*, Farrokhi and Kristiansen [2016]. Figure 4.2 shows the typical surface appearance of the nitrogen assisted laser cuts after the dross attachments were chipped off. Even though the cutting used pure nitrogen gas, oxidation could not be avoided, especially in the start and stop areas. In general, this type of laser cut exhibited a relatively high quality in terms of perpendicularity and surface roughness. However, the results of surface roughness measurements showed a relatively high standard deviation.

In general, the cut surface consisted of three different zones.

- Zone 1 was relatively the smoothest zone with the average surface roughness (R_a) value of about 16 μm. However, the global peak values were relatively high, meaning that the kerf width was locally narrow at this part. The depth of this zone was approximately limited to the first 3-5 mm upper side of the cut edge.
- Zone 2 exhibited a relatively steady surface quality with typical vertical laser cutting striations. The average surface roughness (R_a) value of this zone could be as high as about 28 μm.
- Zone 3 consisted of a more chaotic pattern of striations with the highest average surface roughness (R_a) value of about 30 μm.

The typical groove shape in a I-butt joint configuration can be seen in

Figure 4.3. The groove shape (c) was obtained by a microscopic measurement that has been explained in **Paper 1**. It should be noted that the imgae (c) has been unscaled and magnified for a better presentations. As was mentioned previously, according to the surface roughness measurement results, zone 1 exhibited relatively higher global peak values, that resulted in an almost zero gap in the upper 5 mm of the butt joints.

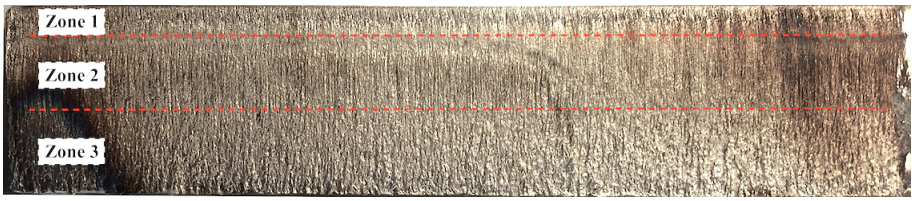

Fig. 4.2: Surface appearance of nitrogen assisted laser cuts: 60 mm/min travel speed and 3 kW laser power (120 mm length).

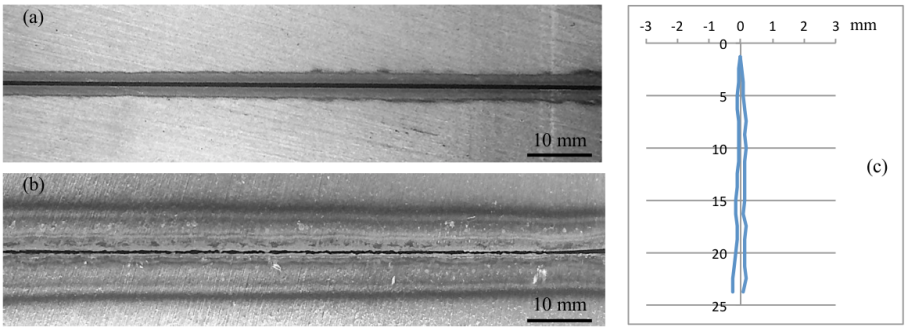

Fig. 4.3: Butt joint configuration formed by the nitrogen assisted laser cut plates (100 mm length): (a) top side, (b) bottom side, and (c) microscopically measured groove shape (magnified and unscaled), Farrokhi et al. [2015a].

4.2.2 Oxygen assisted laser cutting

A thorough explanation of the quality characteristics of oxygen assisted laser cuts and the corresponding cutting procedure has been presented in **Paper 3**: *Single-Pass Hybrid Laser Welding of 25 mm Thick Steel*, Farrokhi et al. [2017]. Figure 4.4 shows the typical surface appearance of the oxygen assisted laser cuts after the dross attachments were chipped off. As it was expected, the cut surface was covered by oxide layers due to the reactive assist gas that was used in this process. The instabilities during the start and stop parts of the process resulted in deep striations in these areas. Apart from that, the cut surfaces typically exhibited a relatively smooth roughness with an average (R_a) value

of about 7 μm. In addition, as shown in Figure 4.4, the striations were highly inclined due to the high cutting speed of 680 mm/min that was 11 times faster compared with the nitrogen assisted laser cutting. However, such high speed cutting could be obtained at the cost of a narrower process parameter window and a poor perpendicularity compared with the nitrogen assisted laser cutting. In addition, in laser cutting with oxygen assist gas the process reproducibility was significantly lower compared with laser cutting with nitrogen assist gas. This resulted in less perpendicularity and an increase in the average surface roughness (R_a), for example, up to about 34 μm in some cases.

The typical groove shape in a butt joint configuration can be seen in Figure 4.5. As shown in Figure 4.5 c, the cut surfaces formed a special *tulip-shaped* groove in the butt joint with a 6 to 8 mm long root face. However, the dimensions of the groove varied slightly in different sections of the specimens, even though the kerf shape remained more or less the same. Table 4.1 summarizes the comparison between the two laser cutting methods that was performed using a 3 kW single-mode fiber laser.

Fig. 4.4: Surface appearance of oxygen assisted laser cuts: 680 mm/min travel speed and 3 kW laser power (120 mm length).

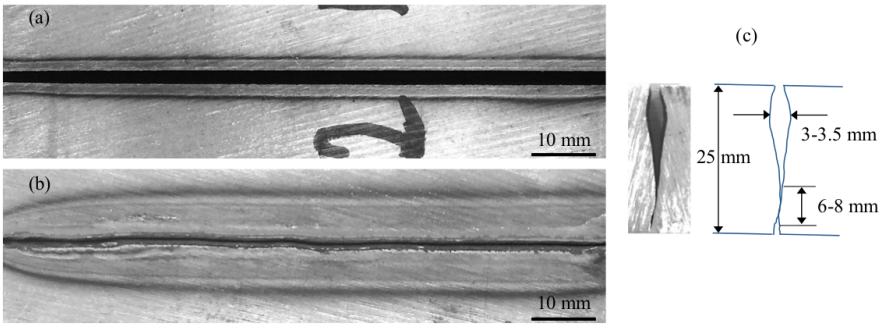

Fig. 4.5: Butt joint configuration formed by the oxygen assisted laser cut plates (100 mm length): (a) top side, (b) bottom side, and (c) typical groove shape, Farrokhi et al. [2017].

Table 4.1: Qualitative comparison of laser cutting in this study with the different types of assist gas.

	Nitrogen	Oxygen
Cutting speed (mm/min)	50 - 60	680
Dross formation	Yes	Yes
Oxidization	Mainly at start/stop	Yes
Perpendicularity	Good	Poor
Groove shape in butt joint	I-groove	Tulip-shape
Average surface roughness Ra (μm)	25 (three zones)	From 7 to 34 in different experiments
Process reproducibility	Highly repeatable	Poor: narrow process window

4.3 Influence of surface roughness

The influence of surface roughness characteristics of laser cuts on the subsequent hybrid laser welding has been experimentally studied in **Paper 2**.

For this purpose, a profilometry technique was used to measure the roughness characteristics of the samples within a 24 mm x 24 mm area. Post-processing and the analysis of the surface measurements used SPIP software. Linear plane correction and Gaussian long wave filtration were applied to the measurements. The extreme noise values were eliminated from the evaluation domain so that the eliminated area did not exceed the 0.5% of the total height distribution area. This has been shown in Figure 4.6 as an example on one of the specimens (milling quality 1).

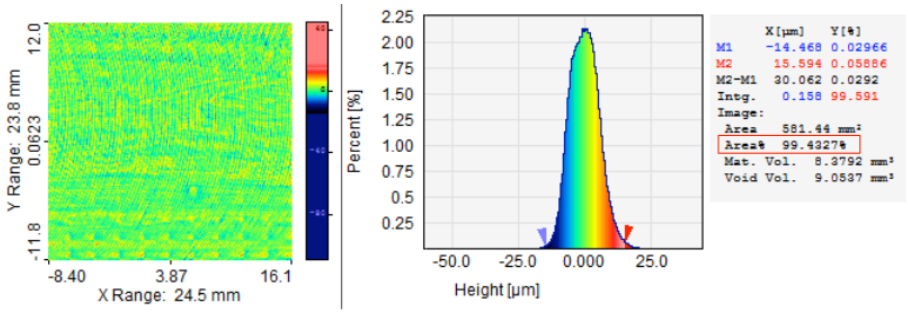

(a) (b)

Fig. 4.6: Analysis of surface quality 1 in SPIP: (a) measurement area, and (b) height distribution graph and the cursors that eliminate the noises from the peak values up to about 0.5% of the total area.

Four different surface qualities were examined in this study. The laser cut samples were compared with three different milled samples each having their own roughness characteristics.

- Milling quality 1: common industrial milling quality for the joint preparation of welding. This surface type had an average roughness (Sa) value of about 4 μm.
- Milling quality 2: rough milling quality with an average roughness (Sa) value of about 9 μm.
- Milling quality 3: rough milling quality with an average roughness (Sa) value of about 30 μm. This type of surface was prepared so that its average roughness (Sa) and root mean square (Sq) values were nearly the same as them in the laser cut surface. This enabled us to investigate the influence of surface patterns namely, (i) the vertical striations of laser cutting and (ii) the systematic tool pattern of milling on the subsequent welding process.
- Laser cutting quality: the typical nitrogen assisted laser cut quality that was presented previously. The cut surfaces were sandblasted to assure that no oxide layer exists.

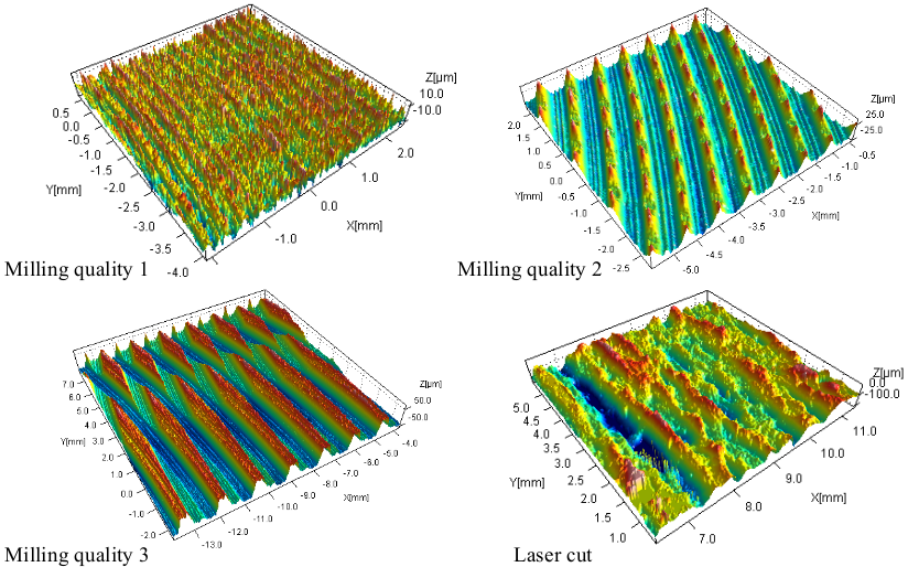

Fig. 4.7: Four different surface qualities used in this study, Farrokhi and Kristiansen [2016]. Note: the color scales are different in each surface. For detailed comparison of the surfaces refer to the original paper (**Paper 2**).

The profilometry of the four surface qualities can be seen in Figure 4.7. Butt joints of 25 mm thick S355J2 steel plates having these surface qualities, as the joint preparation method, were formed and welded using hybrid laser

welding. The characteristics of the butt joint of the laser cut plates has been shown in Figure 4.3. To allow comparison, the same process parameters were applied for each set of experiment. In addition, each set of experiment was compared in different travel speed levels to investigate the process efficiency. Moreover, apart from the main experiments that used zero pre-set gap in the joint preparation, some experiments having surface quality 1 were also carried out with 0.1, 0.3, and 0.5 mm pre-set gaps (see Figure 4.8). This enabled us to investigate the common industrial preparation techniques that use pre-set gap to increase the weld penetration. More information about the experimental procedure can be found in **Paper 2**. The results of the experiments of this study are summarized as following:

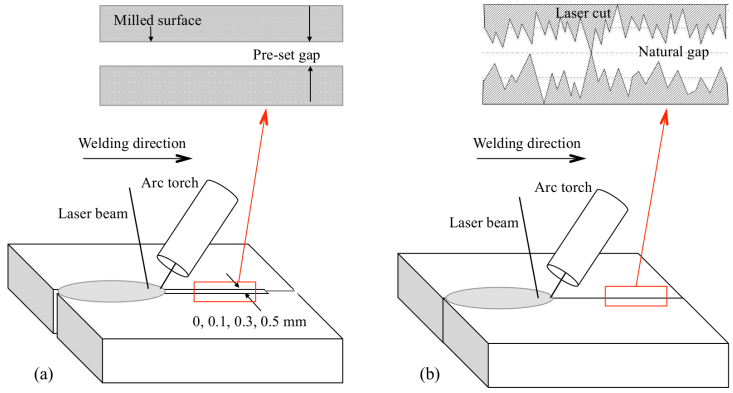

Fig. 4.8: The schematic view of hybrid laser welding of joints prepared by: (a) milling, (b) nitrogen assisted laser cutting.

- Preparation of edge surface quality has a significant influence on the efficiency of the subsequent hybrid laser welding. In comparison with commercial preparation methods with milling, it is possible to achieve up to 130% increase in welding travel speed by using plates with laser cut-edge surface. Figure 4.9, as an example, compares the penetration depth between two welds with the same process parameters, but different preparation methods.

- An approximation of the natural gap caused by the rough striations of the laser cut surface showed that a joint with laser cut edge surfaces and zero pre-set gap has the same gap volume (at its maximum) as a joint prepared using commercial milling methods and a 0.15 mm pre-set gap. This implies that, using the laser cut surfaces allows welding with zero pre-set gap, which makes it easier to position workpieces, while having the benefit of an equivalent pre-set gap at the joint.

- Increase in the average surface roughness, within the range of 9 to 30 μm, cannot solely increase the hybrid laser welding efficiency. In fact, at the higher roughness values, it seems that the effect of surface roughness patterns on the efficiency of the hybrid laser welding process is more noticeable compared with the effect of average surface roughness value alone. In this experiment, the chaotic vertical striations caused by laser cutting could lead to higher welding travel speed compared with the systematic square-shaped pattern caused by milling tool. This could possibly be attributed to a more efficient melt flow or an enhanced laser beam coupling as a results of the laser cut striation pattern. However, further research is required to figure out the exact mechanism of this phenomenon.

- Results of weld quality evaluation in **Paper 2**: Based on the radiographic tests and macro-analysis results, no major porosity was detected. However, solidification cracks were found in the welds, regardless of their surface preparation method (Figure 4.9). Generally, the cracks appeared as discontinuous small indications on the digital radiographic images (will be shown in Chapter 5), and small vertical indications in the laser-dominated area of the macro-sections. In some cases, they were even too small to be detected on digital radiographic images. The cracks characteristics will be explained later in Chapter 5.

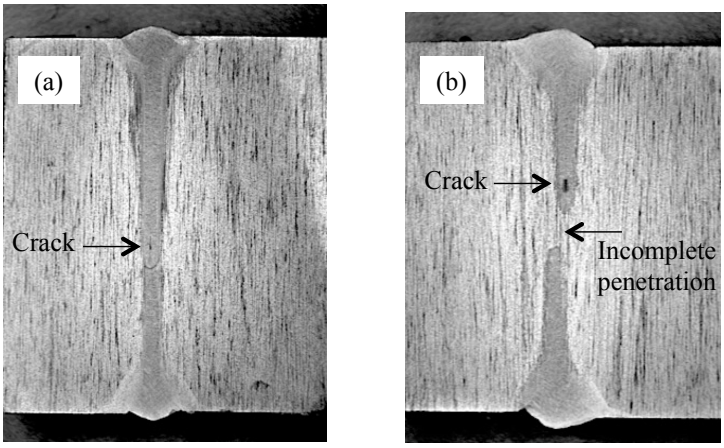

Fig. 4.9: Macrosection (cross section) view of two double-sided welds with the same process parameters (14 kW laser power and 3500 mm/min speed for each pass), but different joint preparation methods: (a) nitrogen assisted laser cutting, (b) milling.

4.4 Influence of groove shape

The influence of groove shape made by laser cutting on the subsequent hybrid laser welding has been experimentally studied in **Paper 1**, **Paper 3**, and **Paper 4**: *Application of Hybrid Laser Arc Welding for the Joining of Large Offshore Steel Foundations*, Kristiansen et al. [2017].

Paper 1 with an industrial point of view, as the first experiment of this thesis, compares the butt joints prepared by different cutting methods. For this purpose, the steel plates were cut by nitrogen assisted laser cutting, plasma cutting, abrasive waterjet cutting, and their characteristics such as cut surface roughness (R_a) and perpendicular tolerance (u) were evaluated. In addition, some plates of the same material were prepared by a commercial milling machine to allow comparison as a reference for the pure I-joint. Double-sided hybrid laser welding was performed on 25 mm S355J2 steel plates, meaning that first, one side was welded and then the sample was turned around to weld the second pass on the other side. The results of this study are summarized as following:

- Aside from the milled surfaces, which had the highest quality in terms of both perpendicularity (only 0.07 mm deviation) and average surface roughness (1.4 μm, R_a), the product of abrasive water cutting had an appropriate balance of surface quality. Laser cutting exhibited a relatively good perpendicularity u_m of 0.22 mm which was comparable with the fine quality abrasive waterjet cutting with the u_m of 0.29 mm. However, the laser cuts had the highest average roughness among the others due to the relatively deep striations of laser cutting. Finally, plasma cutting resulted in the worst quality in terms perpendicularity with the large deviation of 1.2 mm.

- Milled samples as well as cut plates obtained by abrasive cutting, plasma cutting, and laser cutting could be used for the subsequent hybrid laser arc welding process. Nevertheless, each preparation method required a specific set of welding process parameters for obtaining comparable and sound joints.

- Abrasive waterjet cutting as a preparation method can be substituted with milling as their subsequent weld properties were identical for the same set of welding parameters.

- The low perpendicularity of plasma cuts resulted in an asymmetrical V-shape grooves at the butt joints. Therefore, a 60% increase of the filler material was required to fill the gap during welding.

- Nitrogen assisted laser cutting as the preparation method resulted in about 20% less laser power consumption for welding compared to water

jet cut and milled samples with the same joint assembly. This was the basis and motivation for **Paper 2** that was explained in Section 4.3. Notably, this phenomenon was first reported in Farrokhi [2014] during experiments on laser welding of ultra high strength steels, Farrokhi et al. [2015b], and was suggested for future studies.

- Results of weld quality evaluation in **Paper 1**: Based on the radiographic tests and macro-analysis results, no major porosity was detected, except for the welds with plasma cut preparation that had a few pores. However, solidification cracks were found in the welds, regardless of their surface preparation method.

Another study that has been presented in **Paper 3**, investigated the influence of oxygen assisted laser cutting, as the preparation method, on the subsequent hybrid laser welding. In this study, the laser cut plates were sand-blasted and then positioned to form a butt joint as shown in Figure 4.5. To avoid the melt pool dropping through the joint, ceramic backing strips were placed at the root side. Further information on the experimental procedure can be found in **Paper 3**. According to the results of this study, the use of oxygen assisted laser cut plates enabled a special groove shape to be obtained that made it possible to perform a single-pass welding of 25 mm thick steel using only 14 kW laser power. In addition, no crack and porosity was found in the welds. However, as the groove shape dimensions tended to vary slightly from sample to sample (Figure 4.5), the process was not completely reproducible, and lack of penetration together with weld solidification cracking occurred in some experiments. This was an important observation for the research objective 2 which will be discussed later in the next Chapter.

In an attempt for obtaining crack-free welds using a two-pass welding technique, **Paper 3** followed the **Paper 2**'s suggestion and partly employed the nitrogen assisted laser cutting for the preparation of Y-grooves. For this reason, the laser cut plates were beveled on the top side to form the Y-shape in butt joint, so that the root face had the laser cut surface characteristics. Figure 4.10 shows a sample that was prepared this way. To allow comparison, some samples were prepared with the milled root face surface. A two-pass welding procedure was applied, meaning that first, the root face was welded by hybrid laser welding, and then an arc welding pass filled up the groove.

In general, the quality of the welds were acceptable and no internal defects were detected according to the radiographic test results. Nevertheless, in the case of the samples prepared by milling, the weld toe angle at the root side was relatively small (about 120°) and the excess penetration was about 2.3 mm (see Figure 4.11 b), leading to the weld quality level c according to ISO 5817:2003 standard for arc welding. Optimization of the weld toe angle (shape) and the excess penetration at the root side using different welding speed was not possible. For instance, a 20% reduction of welding speed led to a wider

root weld but did not increase weld toe angle at the root. Similarly, increasing the welding speed by up to 20% either resulted in extremely unsteady root humping or incomplete penetration. However, as shown in Figure 4.11 c the samples whose root faces were prepared by low-speed laser cutting yielded higher quality at the root side. Using such preparation method not only allowed welding with higher travel speed, but also a very smooth and steady root weld could be obtained. Although the weld toe angle of 140° was yet below the the requirement of the quality level b (150°), the excess penetration of 0.6 mm was small enough to meet the quality level b requirements according to ISO 5817:2003 standard. The modified experiment shown in Figure 4.11 c used the same welding parameters, except for the welding speed, which was 300 mm/min faster than the other experiment (in Figure 4.11 b) owing to the nitrogen assisted laser cutting method adopted for preparation.

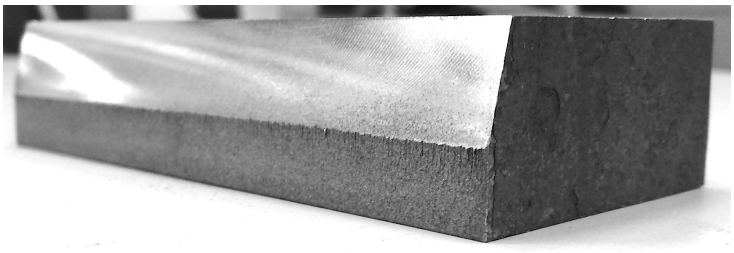

Fig. 4.10: Plates were cut by laser, sandblasted, and then beveled to form Y-shape in the butt joint.

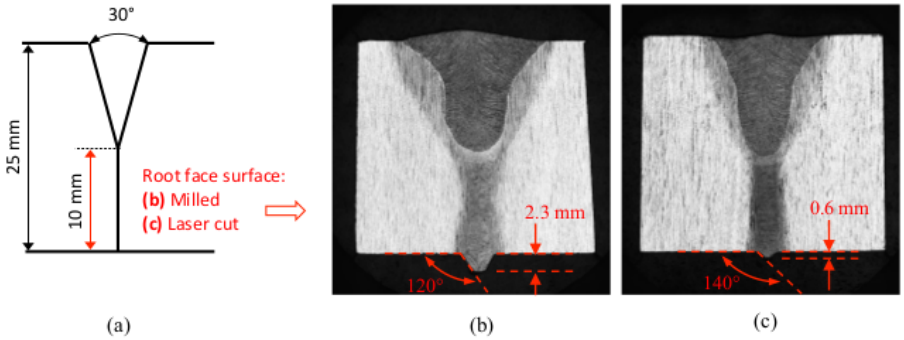

Fig. 4.11: (a) Groove geometry for two-pass welding. Cross-section of the welds: root face prepared by (b) milling and (c) nitrogen assisted laser cutting as shown in Figure 4.10, modified after Farrokhi et al. [2017].

Finally in the last set of experiments for this section, **Paper 4** investigated positional hybrid laser welding of steel parts related to suction bucket foundation components. Large and heavy structures such as offshore steel foundations

demand positional welding processes, as the manipulation of such heavy parts is unpractical. Therefore, this study provided a number of preliminary positional welding experiments using robotized hybrid laser welding. As shown in Figure 4.12 different sections of two skirt segments with a plate thickness of 16 mm were used for the investigation. The purpose of the study was to test the performance and quality of (i) different joint types with minimal joint preparation and (ii) different welding positions which could possibly be used for the production of the bucket skirt. Detailed information can be found in **Paper 4**. According to the results of this study some points can be highlighted as following:

- The semi-Y-shape flat positioned groove of the bended section allowed a high amount of filler material to be deposited inside the joint. It resulted in about 23 mm penetration of the root weld with 16 kW laser power.
- The flat welding position showed a sufficient penetration for the butt joints. For the lap joints, the penetration depth and width of the weld at the intersection between the plates to a very limited extent resulted in acceptable welds. This can be explained by the fact that the available laser power could not provide a sufficient penetration depth.
- The vertical welding position was significantly less stable compared with the flat welding position for the same process parameters. A lower power input and a higher travel speed were required in order to avoid the melt pool from collapsing when welding in the vertical position.
- This paper did not include radiographic test, however, solidification cracks were randomly detectable in the macro-section of the welds.

Fig. 4.12: (a) The hybrid laser welding setup for vertical welding position. (b) Skirt parts before welding and (c) after welding in several positions.

4.5 Conclusion and suggestions

4.5.1 Addressing the research objectives

Before closing the chapter, the specific research questions related to the research objective 1 will be answered in this section.

What is the influence of the cut surface roughness (from laser cutting) on the quality and efficiency of the subsequent hybrid laser welding?

In comparison with commercial preparation methods with milling machines, using plates with nitrogen assisted laser cut-edge surface provides the following benefits:

- It is possible to increase the travel speed of the root welding.
- It allows welding with zero pre-set gap, which makes it easier to position workpieces. This is because the natural gap caused by the rough striations of the laser cut surface compensates for the lack of pre-set gap.
- It is possible to obtain welds with higher quality and stability at the root side.

What is the influence of the cut kerf (from laser cutting) on the quality and efficiency of the subsequent hybrid laser welding?

In comparison with commercial preparation methods with milling machines, using plates with nitrogen assisted laser cut-edge surface can provide an acceptable perpendicularity level that has almost no negative effect on the subsequent welding process. Using plates with oxygen assisted laser cut-edge surface may result in highly curved shapes at the edge that reduces the repeatability of the subsequent welding. However, in some cases, the tulip-shape groove enabled an increase in penetration depth and allowed welding of 25 mm plates in one single-pass.

From an industrial point of view, can the laser cutting be adapted as the joint preparation method for the subsequent hybrid laser welding? If yes, what are the quality and efficiency advantages?

Yes, considering the above mentioned points, an integrated laser cutting-welding system can be used to increase the quality and efficiency of the subsequent hybrid laser welding process. In addition, such system allows more flexibility during the manufacturing. For instance, in the same cutting unit, it is possible to provide different joint preparations and groove shapes for the

subsequent welding process by using simply different cutting parameters and setups.

4.5.2 Suggestions for laser cutting-welding integration

Based on the results of experiments in this study, two laser units may be used to increase the quality and efficiency of the hybrid laser welding process. Figure 4.13 depicts an example of an integrated laser cutting-welding system for the welding of two types of butt joints. It is important to note that, as was mentioned in Section 4.1, the cutting and welding experiments used different laser types in this study. Changing the laser type, for example, using the disc lasers of LWT for both cutting and welding may lead to different results and qualities.

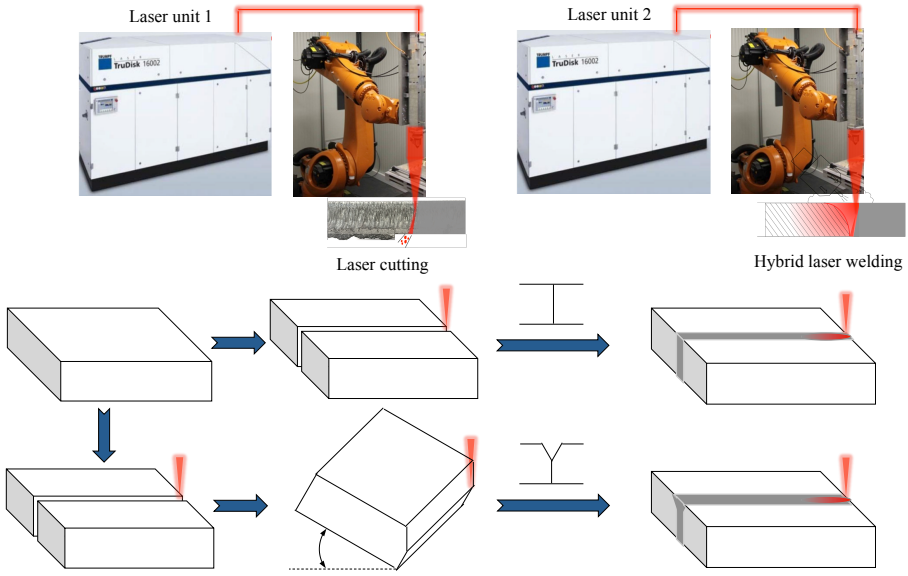

Fig. 4.13: An integrated laser cutting-welding system for two types of butt joint welding.

Chapter 5

Avoidance of solidification cracking

In this chapter, the summary of investigation that has been performed to address the research objective 2 will be presented. The chapter consists of two main sections. First, Section 5.1 will discuss the experimental observations and will mainly include the researches that have been presented in **Papers 1-3** and **Paper 5**. Following these observations and the elaborations on the solidification cracking behavior, the chapter will continue by Section 5.2, which presents the numerical modeling of the welding experiments in order to support the interpretations of the study. This section will be based on the research that has been carried out in **Paper 5** and **Paper 6**. Finally, the general conclusions will be drawn in the last section.

5.1 Experimental observations

5.1.1 Double-sided welds

Parallel to the previous analysis that mainly intended addressing the research objective 1 questions, every welded specimen (except in **Paper 4**) was subjected to the radiographic test to obtain as much information as possible in relation to the solidification cracking phenomenon (research objective 2). In general, the results of the x-ray tests and the macro-analysis of the welding experiments in this study, confirmed that the avoidance of weld solidification cracking is one of the main challenges in hybrid laser welding of thick-section S355J2 steel. A wide range of welding heat inputs, travel speed, and laser power with different welding setups were applied during the double-sided (partial penetration) welding of 25 mm butt joints. For example, line energy values for each welding pass varied from the maximum of 2 kj/mm in **Paper 1** to the minimum of 0.33 kj/mm in **Paper 2**. However, solidification cracks could not be avoided in the welds yet. A total of 48 cracks that were detected in the weld specimens of **Paper 1** and **Paper 2** have been reported in the following text. It should be noted that some of the replicates, faulty experiments, and the experiments that were difficult for interpretation, were excluded from the analysis due to time limitation and also to increase the reliability of the

study. Moreover, this report includes all the welding experiments that used 14 kW laser power for each pass and had different surface preparation and pre-set gap.

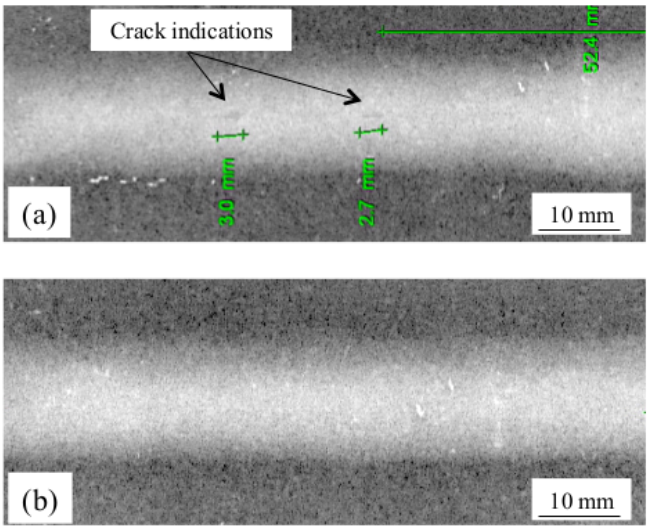

Fig. 5.1: Examples of x-ray radiographic images (welding parameters: 14 kW laser power and 500 mm/min speed for each pass): (a) a weld with two cracks, (b) a crack-free weld.

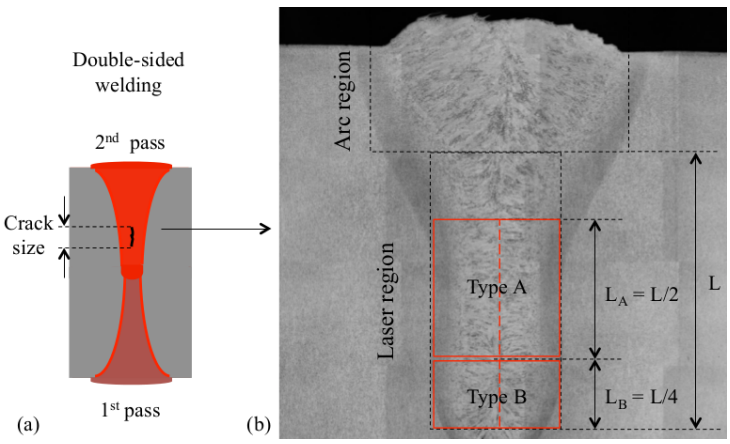

Fig. 5.2: (a) Schematic of the double-sided welds and the crack size definition in this study. (b) Susceptible zones for type A and type B cracks on the centerline of each pass.

In general, the cracks were not continuous and occurred once or several times along the welding direction (see Figure 5.1). In some cases, the length of the cracks could be as short as 0.5 mm, which made them difficult to be

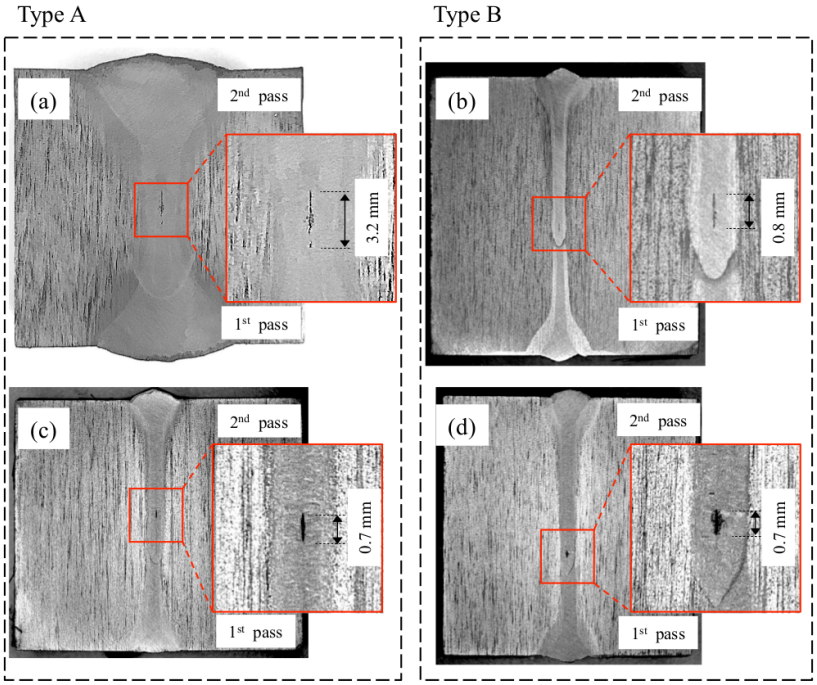

Fig. 5.3: Two types of cracks detected in the double-sided welds: Type A: in the mid-section of the laser dominated region, Type B: in the root-section of the laser dominated region. Parameters for each pass: 14 kW laser power and the travel speed of (a) 500 mm/min, (b) 4700 mm/min, and (c and d) 2300 mm/min.

captured on the digital radiographic images. Therefore, the study of crack size in the longitudinal direction would not yield a reliable report. For this reason, as shown in Figure 5.2 a, the crack size was investigated in the depth direction on the weld cross-sections. Almost in all cases the cracks appeared on the weld ceneterline somewhere in the depth of the laser dominated region. As can be seen in Figures 5.2 b and 5.3 two types of cracks were detected in terms of their location in the welds. If the length of the laser dominated region in a weld is equal to L, then the crack types could be defined as following:

- *Type A* cracks appeared in the mid-section zone of the laser-dominated region within a length of L/2. This type of crack tended to have relatively larger size (up to 3.4 mm long) and therefore, it was easier to be detected on the digital radiographic images. Despite that, in some cases as in Figure 5.3 c, the crack could be relatively small.

- *Type B* cracks appeared in the root-section zone of the laser-dominated region within a length of L/4. This type of crack was limited in size and could be 1 mm long at its maximum. In some cases, they did not appear

on the digital radiographic images and were only detectable during the macro-analysis of the weld cross sections. Such cracks may also be called *flaw* due to their small size. However, in a few cases cracks also appeared in both A and B zones.

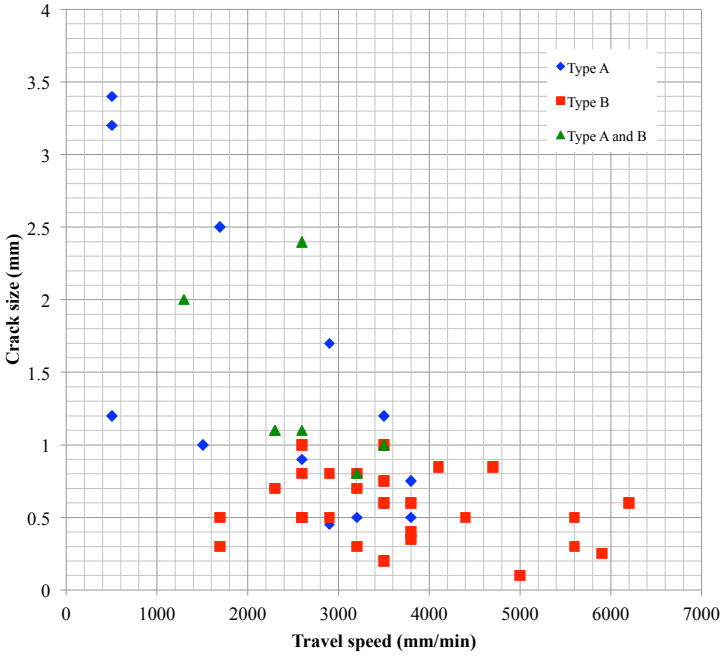

Fig. 5.4: Correlation between the crack size (as per Figure 5.2) and the welding travel speed. Double-sided welding experiments: 14 kW laser power for each pass (Data adapted from [Farrokhi and Kristiansen, 2016; Farrokhi et al., 2015a]).

Figure 5.4 depicts that a correlation exists between the crack size and the welding travel speed or the laser heat input. The higher the travel speed, the smaller the cracks tend to be. It is also evident from the data that the crack type shifts from B to A as the travel speed decreases, in this case, below 1700 mm/min. Within the speed range of 1700 to 3800 mm/min the both types of cracks can be seen in the data. This has been shown for example, in Figure 5.3 c and d, that in two different experiments having the same travel speed, cracks had the same size, although any of A or B types could occur in the welds.

However, it is of great importance to note that, this data does not represent the probability of cracking, that is the travel speed or heat input did not clearly influence the chance of cracking in this range of experiments.

Although these experiments were not systematically designed for this purpose, yet their results can roughly suggest that weld solidification cracking

phenomenon is too complex to be avoided solely by the control of heat input. Furthermore, the fact that all of these welds were double-sided, meaning that each joint consisted of two partial penetration welds, draws one's attention to the role of the newly raised subject of penetration-mode. This was one of the main motivations for planning the one-sided welding, in which the hybrid laser welding takes the advantage of full penetration-mode in welding.

5.1.2 One-sided welds

Two motivations were associated with planning for one-sided welding. (i) The results of double-sided welding experiments in a wide range of travel speed was not satisfying. Additionally, as discussed previously, the literature review reveals that despite the importance of the subject, only a limited number of studies have related the effect of penetration-mode and the design of weld sequences to the chance of cracking and more systematic investigations are required. For this reason, **Paper 3** aimed at developing two different procedures for crack-free welding with a special attention to the penetration-mode effect. (ii) Steel plates with such thicknesses (e.g. 25 mm) are often used for the manufacture of large and heavy structures, limiting the possibilities for the manipulation of such parts during the welding process. Therefore, the second motivation for one-sided welding in **Paper 3** was to minimize the need for the manipulation of parts.

Following the argument on the possible negative effect of partial penetration-mode on the occurrence of solidification cracking, the one-sided welding experiments were designed so that only a single-pass hybrid laser weld was used for joining the plates. This technique allowed obtaining full-penetration mode, meaning that there was no solid material below the root-section of the hybrid laser weld.

Two-pass welding

One way of making one-sided welds was to use the hybrid laser welding only for the root pass of Y-groove butt joints. Following the root pass, the groove could be subsequently filled up by a MAG welding pass. According to the results, a shallow and continuous solidification crack appeared in some cases on the weld bead surface of the root welds. In contrast with the type A and B cracks that occurred in the double-sided welds, these cracks were continuous and they appeared along the weld bead surface. Such surface cracks that are typical in the conventional arc welding as well, are far less challenging compared with the ones that are formed in the depth of the laser dominated region. This is due to the fact that surface cracks can be healed by the subsequent filling passes, if they are shallow enough to be re-melted. In this experiment, the cracks were generally shallow and the deepest was measured as 1.6 mm long, so the cracks

could be re-melted and healed during the second pass. The macrographs and x-ray tests revealed no cracks in the final welds of three replicates, and the experiments were 100 % repeatable.

Single-pass welding

The other way of making one-sided welds was to use the oxygen assisted laser cutting for preparation of the joint. As it was explained in Section 4.4, the use of oxygen assisted laser cut plates enabled a special groove shape to be obtained that allowed single-pass welding of 25 mm thick steel using only 14 kW laser power. More importantly, neither crack nor porosity was found in the welds. However, as the groove shape dimensions tended to vary slightly from sample to sample (Figure 4.5), the process was not completely reproducible, and lack of penetration together with weld solidification cracking occurred in the partial penetration experiments. The cracks could be categorized as type A in the mid-section of the laser-dominated region with an average size of 2 mm.

Although these welds had a poor reproducibility and they could not be employed in the real-life welding tasks, understanding the reasons of such observations could be of great importance in comprehending solidification cracking phenomenon. The fact that the partial penetration experiments were associated with solidification crack in the weld, is evident to the role of penetration-mode in the occurrence of weld solidification cracking as the both experiments used exactly the same process parameters. A closer look into the microstructure of the welds in the crack susceptible regions (type A zone) revealed that the grain structure could be different depending on the penetration-mode. The microstructure of partial penetration welds consisted of acicular ferrite and bainite, and the solidification mode was cellular or dendritic (epitaxial) with the typical columnar growth from the sides to the weld centerline. Similarly, the full penetration welds consisted of acicular ferrite and bainite in the microstructure, but in this case the solidification mode was equiaxed dendritic in some cases.

Recently, Wahba et al. [2016] also observed the same grain structure in the welds of 25 mm thick SM490 steel plates that were welded using their newly-developed single-pass hybrid laser welding technique with cut wires and backing. Their results have been compared with the results of this experiment in Figure 5.5. However, they did not provide any explanation for the cause of their observations in Wahba et al. [2016]. This study therefore, attempted to provide possible explanation on these observations. For this reason, a new set of experiments was carried out for investigating the effect of penetration-mode on the weld characteristics and quality. This has been explained in the following section.

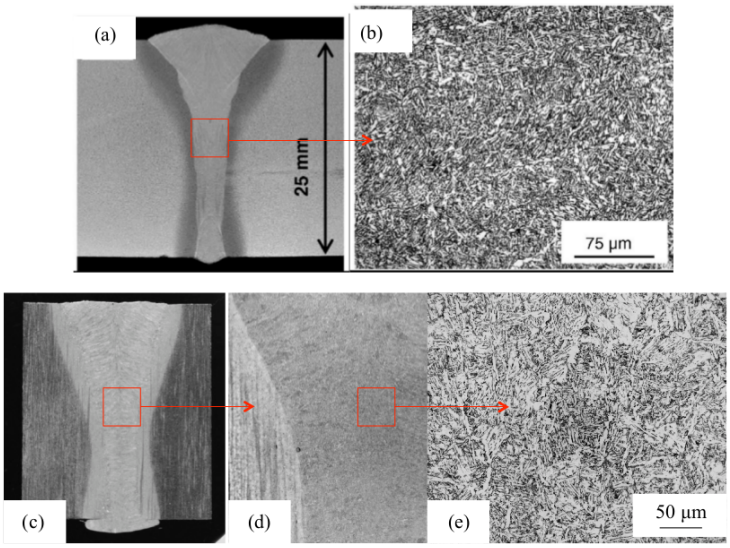

Fig. 5.5: Single-pass hybrid laser weld of 25 mm steel according to (a,b) Wahba et al. [2016] and (c-e) Farrokhi et al. [2017].

5.1.3 Penetration-mode effect

In order to investigate the effect of penetration-mode, the experiments used the same parameters on the same steel plate of type S355J2 with 10 and 25 mm thicknesses. The process parameters were selected for obtaining 10 mm penetration depth in single-pass. This allowed obtaining full and partial penetration welds, in which the welding heat input and penetration depth could be roughly identical. Two replicates were experimented and the samples were subjected to a full-length x-ray test and two macro analysis on random sections. The complete experimental procedure has been presented in **Paper 5**: *A Numerical Model for Full and Partial Penetration Hybrid Laser Welding of Thick-Section Steels*, Farrokhi et al. [2018b].

As shown in Figure 5.6, partial penetration welds were associated with hot cracks. The cracks were perpendicular to the weld and they appeared at the root side. However, according to the macrosections and the results of x-ray tests non of the full penetration welds contained such cracks in the weld. This implies that partial penetration welds were more prone to cracking compared with full penetration welds with the same process parameters. In addition, as stated in **Paper 5**, for the given welding process parameters for 10 mm penetration depth, partial penetration welding exhibited a *bell shape* weld cross section, whereas, full penetration welding resulted in an *hourglass shape* weld cross section that was associated with the extension of the melt at the root. This is evident that thermal cycles and heat distribution could be significantly

different depending on the penetration-mode, despite the fact that the same welding heat input was employed for the both set of experiments.

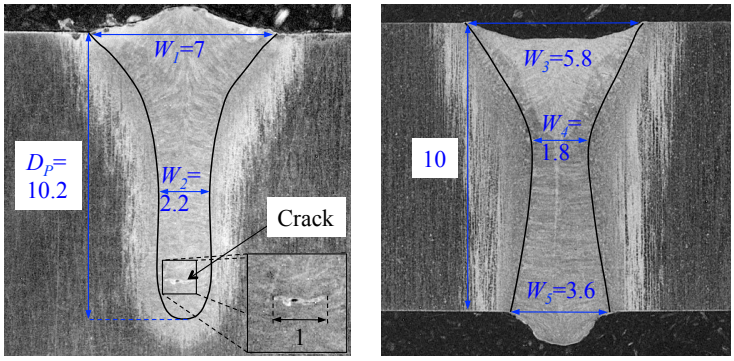

Fig. 5.6: The results of penetration-mode test: (a) partial penetration, (b) full penetration, both used the same process parameters, Farrokhi et al. [2018b]. Note: dimensions are in mm.

As was explained in the review section, two conditions must be met in order for the weld solidification cracking to occur: (i) strain (or stress) and (ii) susceptible microstructure. For the stress factor, according to Gebhardt et al. [2013], the lower local stresses in the full penetration welds of the single-pass welding could have partly reduced the risk of cracking. However, it should be noted that the numerical analysis in Gebhardt et al. [2013] mainly concerned the heat conduction and did not include the effect of the complex melt flow dynamics during the solidification. According to the recent studies made by [Schaefer et al., 2017, 2015], the melt flow dynamics during laser welding may vary depending on the penetration-mode. Accordingly, the local stress distributions at the solidification front may also be induced by the convective melt flows during the welding process. More sophisticated numerical models are required in the future to investigate the stresses induced by the different convective flows depending on the penetration-mode. Concerning the microstructure factor, the formation of equiaxed grains in some cases in the laser dominated region of the full penetration welds, could also promote the resistance to solidification cracking.

As was mentioned in the review section, the subject of grain refinement has been extensively studied in the welding of aluminum alloys and stainless steels. Central to all of these studies, columnar to equiaxed transition (CET) was promoted using one or the combination of these methods: (i) the optimization of solidification and process parameters (Figures 2.4 and 2.5); (ii) the addition of agents that promote heterogeneous nucleation; or (iii) alternative methods such as vibration or magnetic stirring or pulsed heat during welding.

In this study, the latter was ruled out as none of these alternative methods

were used. Moreover, all the single-pass welding experiments used the same process parameters, as well as the same filler material without any deliberate addition of nucleants. Therefore, the possibility of heterogeneous nucleation induced by an external agent from the filler material could be discounted as well. However, as with solidification mechanisms in ingots and castings, equiaxed structures may also occur as a result of dendrite sidearm detachment induced by convection currents in the melt, Porter et al. [2009]. The implication for our study, as was concluded in **Paper 3**, was that a favorable convection current may have occurred during the full penetration welding, leading to the formation of equiaxed structure in the weld centerline. Accordingly, it was possible to confirm the findings of [Schaefer et al., 2017, 2015] that the formation of cracks could be related to melt flow dynamics, which differed in full and partial penetration laser welding.

Nevertheless, the interpretation presented in **Paper 3** was made in the absence of the effect of thermal conditions in the fusion zone. Therefore, the following numerical model was developed in order to provide further knowledge on the thermal conditions of the experiments.

5.2 Numerical modeling of the experiments

In this section, hybrid laser welding with full and partial penetration modes will be modeled for acquiring more in-depth knowledge on the thermal situation of these welds. More specifically, as a results of finding equiaxed solidification mode during the single-pass welding in [Farrokhi et al., 2017; Wahba et al., 2016] (Figure 5.5), this study aimed for calculating the temperature gradients at the solidification front of full and partial penetration welding. In the following section, before the beginning of numerical analysis, the relation between temperature gradients and grain refinement will be described.

5.2.1 Temperature gradients and grain refinement

In metal alloys, apart from the possible influence of the melt flow dynamics, solidification mode can be determined by the combination of chemical composition and two solidification parameters such as temperature gradient of the liquid and solidification growth rate. The two solidification parameters have been mathematically expressed in Equations 2.1 and 2.2, respectively. As was explained in Chapter 2, if the temperature gradient is extremely low, equiaxed dendritic growth can be possible at high solidification rates (see Figure 2.4).

According to [Kou, 2003; Lippold, 2015] solidification growth rate R, can approximately have the following relationship with welding travel speed v:

$$R = v \cdot cos(\alpha) \tag{5.1}$$

where α is the angle between the welding direction and the normal direction of the solidification front. As shown in Figure 5.7 the maximum growth rate of solidification occurs on the weld centerline at the weld pool tail, where α is 0. At this point, the temperature gradient reaches its minimum value and leads to a situation that is potentially suitable for the formation of equiaxed grains.

In two different welding experiments that have the same travel speed v, solidification growth rate R can be assumed to be equal. Consequently, it can be assumed that the temperature gradient G is the main factor that can determine the solidification mode in the weld centerline. This was the main motivation for the numerical analysis in this study based on the scope and objectives that are described in the following section.

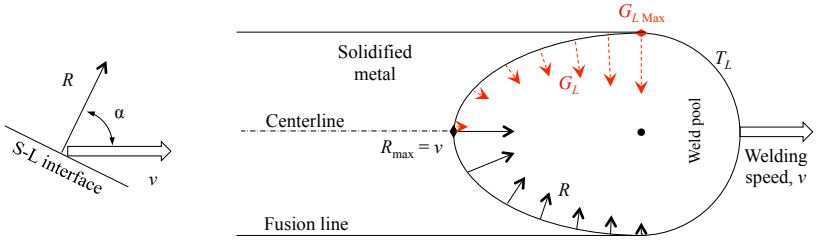

Fig. 5.7: Solidification growth rate R and temperature gradient G_L in the melt pool, modified after Lippold [2015].

5.2.2 Scope and objectives

The aim of the numerical analysis in this study was to provide a comparative study between the full and partial penetration welds having the same process parameters. The numerical analysis, based on 3D transient thermal conduction heat transfer, aimed for calculating the temperature distribution and thermal gradients at the solidification fronts (G_L) using the Finite Element (FE) method. For this reason, first a numerical model for the experiments described in Section 5.1.3 was developed which is presented in **Paper 5**, Farrokhi et al. [2018b]. Then, using this model, the temperature gradients were calculated as shown in Figure 5.8. The results were analyzed and presented in **Paper 6**: *Temperature Gradients at the Solidification Front of Deep Hybrid Laser Welds*, Farrokhi et al. [2018a]. The numerical analysis was based on several assumptions and simplifications that have been stated in the above mentioned papers.

In the following sections, first the numerical calculation of temperature distributions are briefly described, and then, the temperature gradients analysis are presented and discussed.

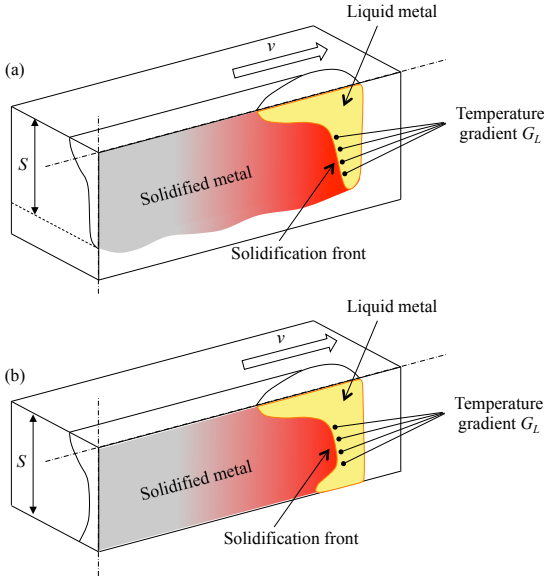

Fig. 5.8: Schematic of the two study cases for the temperature gradient analysis in: (a) partial penetration welding (b) full penetration welding, both on the same material and using the same process parameters. The figure schematically depicts the temperature gradient measurement points at the solidification front of the welds, Farrokhi et al. [2018a].

5.2.3 Calculation of temperature distribution

In order to analyze the temperature gradients, first, the temperature distributions must be calculation. As the FE method was not the main objective of the PhD thesis, this subject was not included in the literature review. However, some fundamentals and reviews of welding simulation in general, can be found for example, in [Dal and Fabbro, 2016; Lindgren, 2006; Mackwood and Crafer, 2005; Rao et al., 2011].

According to **Paper 5** several laser welding experiments have been modeled successfully in the literature using thermal conduction heat transfer, or the so called "thermo-mechanical" (Dal and Fabbro [2016]) models. However, these models have been mainly focused on partial penetration welding. None of these models consider the root widening that often occurs in the case of full penetration welding and results in the formation of an *hourglass* shape weld in the transverse cross section (Figure 5.6b). Therefore, a new boundary condition was required for the modeling of full and partial penetration hybrid laser welding. This was accomplished using LS-DYNA (971 R10) FE code. The detailed description of the model can be found in **Paper 5**. Further details about the numerical calculations and the thermal solver in LS-DYNA can be found in LSTC [2017]. In the following text, the summary of the numerical

modeling is presented.

The temperature distributions were calculated using the classical Fourier's heat equation for 3D transient heat conduction. This equation in a non-linear form (temperature-dependent material properties) is given by the following governing partial differential equation:

$$\rho c(T)\frac{\partial T}{\partial t} = \frac{\partial}{\partial x}\left(k(T)\frac{\partial T}{\partial x}\right) + \frac{\partial}{\partial y}\left(k(T)\frac{\partial T}{\partial y}\right) + \frac{\partial}{\partial z}\left(k(T)\frac{\partial T}{\partial z}\right) + q_v \qquad (5.2)$$

In the above equation, T is the temperature; x,y, and z represent space coordinates; t represents time; ρ represents density, $c(T)$ and $k(T)$ represent temperature dependent specific heat capacity and thermal conductivity, respectively, and finally, q_v is the volumetric internal energy generation that was applied by a hybrid heat source model with a specific boundary shape. As the calculation of the melt flow dynamics is excluded in the thermo-mechanical models, using such volumetric heat sources allows partly compensating for the excluded convective heat transfer that is induced by melt flow in the fusion zone, Dal and Fabbro [2016].

As illustrated in Figure 5.9, the hybrid heat source used in this study, consisted of a double-ellipsoidal heat source proposed by Goldak et al. [1984] for the arc part and a *double-conical* heat source for the laser part that was developed in **Paper 5** based on the previously proposed three dimensional conical (TDC) heat source by Wu et al. [2006]. The double-conical heat source is in fact, an extended version of the TDC, which was proposed for the modeling of plasma keyhole welding. However, TDC heat source - in its original form - was not capable of accounting for the root widening of the full penetration welds. The addition of a reverse cone in the double-conical heat source allowed the modeling of hourglass shaped full penetration welds. Moreover, as shown in Figure 5.10, manipulating the r and z parameters of the double-conical heat source, provides different configurations including the original TDC as well.

In addition to the 12 geometrical parameters of the hybrid heat source, two heat partition factors (β_a and β_l) were defined in the heat source model that have been described in **Paper 5**. These parameters provided a high degree of flexibility in the heat source that facilitated the adaptivity of the model with respect to the experiments.

Moreover, other boundary conditions including heat losses due to radiation and convection were added to all surfaces of the FE model. The model was validated with respect to the temperature measurements in N.Nguyen et al. [1999] and the results were acceptable.

Finally, the model was calibrated for three experimental cases separately. These cases include the penetration-mode experiments in this study (Figure 5.6), as the main interest of the research, as well as the experimental result of an external study by Frostevarg and Kaplan [2014]. The latter was added to

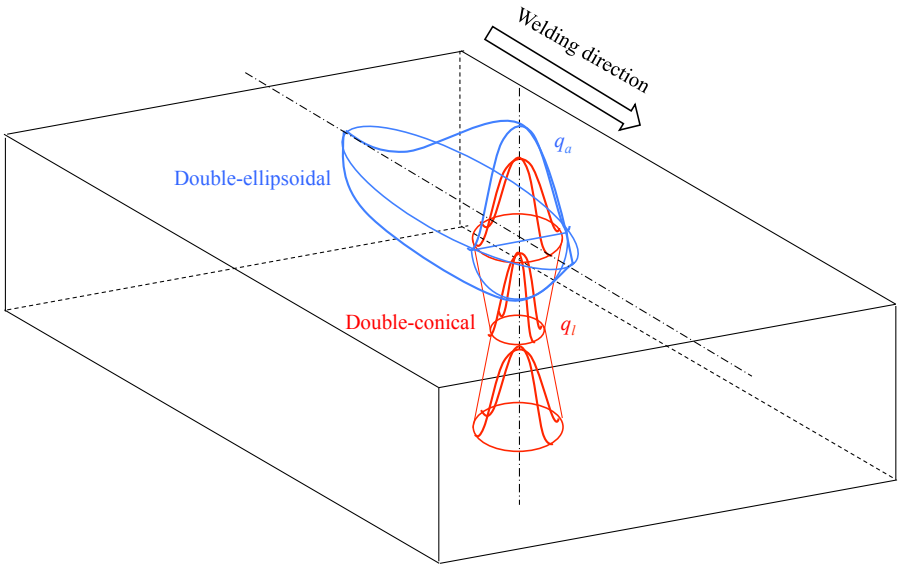

Fig. 5.9: Schematic of the volumetric hybrid heat source used for the modeling (for illustration only). q_a and q_l denote the heat flux by arc and laser, respectively.

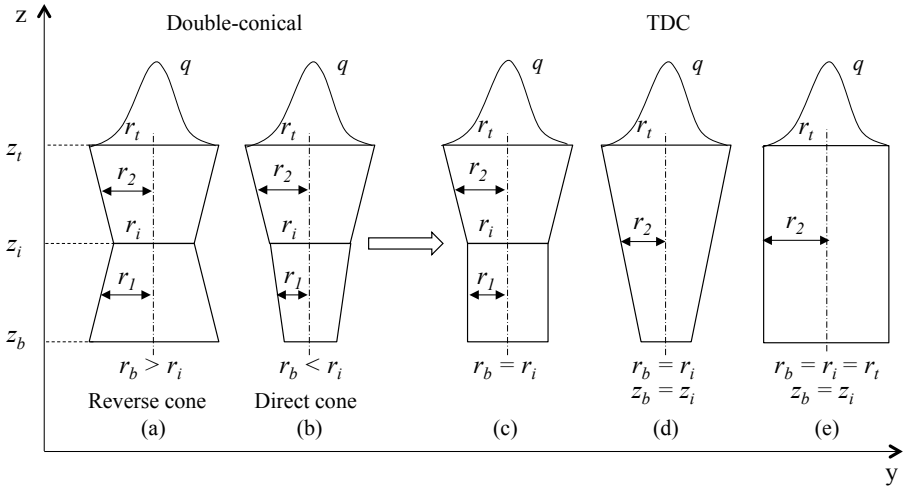

Fig. 5.10: Double-conical heat source with reverse and direct cone configurations and its simplified versions, Farrokhi et al. [2018b].

the investigation in order to evaluate the capability of the model in accounting for the common weld geometries obtainable in the transverse cross section of hybrid laser welds, Farrokhi et al. [2018b]. The three cases were defined as follows:

- Case I: Partial penetration (Figure 5.6a)
- Case II: Full penetration: wide root (Figure 5.6b)
- Case III: Full penetration: thin root (Figure 10a in Frostevarg and Kaplan [2014])

As presented in **Paper 5**, the results of numerical modeling were in fairly good agreement with the experiments. Using the double-conical heat source in the hybrid model allowed the modeling of three common weld transverse cross section geometries that are obtained by hybrid laser welding of thick-section steel. Reverse cone configuration (Figure 5.10a) with different parameters was used for the modeling of full penetration welds. For the partial penetration weld, the typical cone and cylinder configuration was employed to obtain the bell shape weld cross section. This was possible simply by applying the $r_b = r_i$ condition on the double-conical heat source (Figure 5.10c).

The calculated temperature distributions have been shown for the fusion zone of Cases I, II, and III in Figures 5.11, 5.12, and 5.13, respectively. The results are evident that the hybrid heat source presented in this study, is capable of modeling partial penetration welding as well as the root extension that occurs during full penetration laser welding [Frostevarg, 2018; Haug et al., 2013; Powell et al., 2015]. Detailed description of the heat source parameters and the comparison of numerical and experimental results can be found in **Paper 5**.

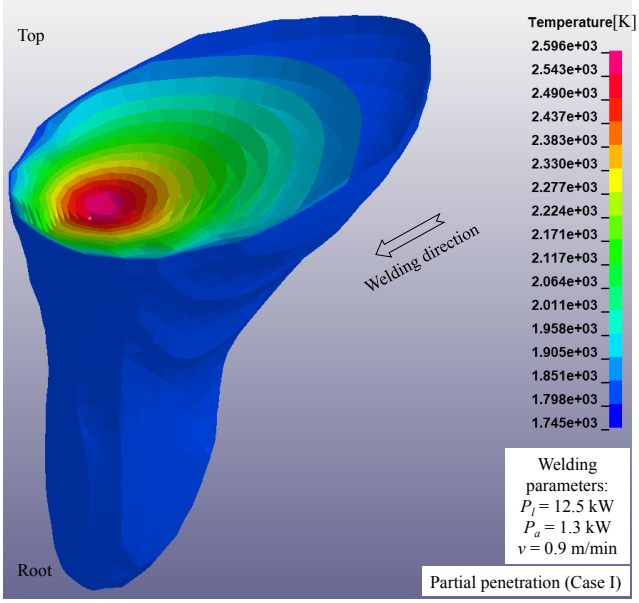

Fig. 5.11: Isometric view of the melt profile: Case I (the experiment in Figure 5.6a).

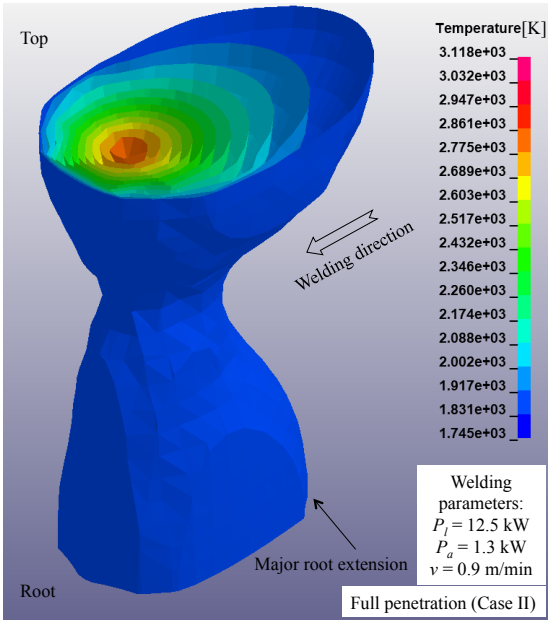

Fig. 5.12: Isometric view of the melt profile: Case II (the experiment in Figure 5.6b).

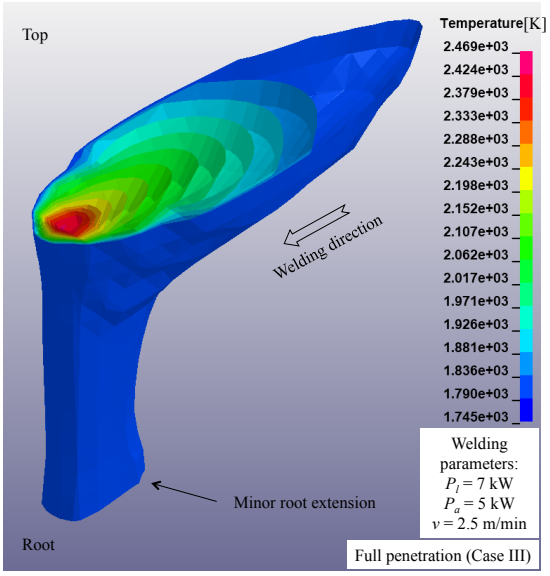

Fig. 5.13: Isometric view of the melt profile: Case III (the experiment in Figure 10a in Frostevarg and Kaplan [2014]).

5.2.4 Temperature gradients analysis

The temperature data obtained by the numerical model, presented in the previous section, were used for the calculation of temperature gradients (G). Only a plane in the centerline of the plate (along the welding direction) was considered in the calculation of gradients (Figure 5.8). To do so, the temperature data of the given times were exported from LS-DYNA and processed in Matlab (R2017b). Calculating the temperature gradients used Sobel operator, Moeslund [2012], which consists of two 3×3 kernels convolving with the temperature data to calculate the approximations of the derivatives, one for horizontal changes, and one for vertical. Further details can be found in **Paper 6**.

The magnitudes of temperature gradients of the liquid (G_L) within the isotherms of solidus and 1795 $^{\circ}K$ temperatures were compared for the both full and partial penetration welds (Figure 5.6) in different depths. The results showed that the full penetration weld exhibited lower temperature gradients compared with the partial penetration weld. However, the difference between the gradients in full and partial penetration welds increased as the depth increased towards the root side of the fusion zone. This was attributed to the fact that the root of the full penetration weld was insulated on one side by the air and was less effectively cooled by the solid metal. As a result of this situation, the isotherms on the longitudinal section of the full penetration welding tended to maintain roughly parallel, and thereby the temperature gradients did not increase at the root side. In contrast, the distance between the isotherms in the partial penetration welding decreased towards the root side as the depth increased.

As explained in **Paper 6**, the formation of equiaxed grains in the fusion zone is promoted mainly by two factors; (i) heterogeneous nucleation mechanisms, and (ii) a sufficiently long constitutionally undercooled zone in the weld pool Kou [2003]. According to the constitutional supercooling theory (Rutter and Chalmers [1953]), the extent of the undercooled zone is governed by the actual temperature gradients in the liquid G_L in front of the solid-liquid interface. For the arc welding of aluminum alloys, it has been shown in the literature that the temperature gradients at the end of the weld pool can be reduced as the heat input and the welding speed are increased, Kou [2003]. The results of the numerical analysis in this study, however, suggested that for given welding process parameters, the temperature gradients in the depth of hybrid laser welds, can be also influenced by the penetration-mode of the welding. In other words, this implies that the region of constitutional supercooling can be potentially larger in full penetration welding compared with partial penetration welding.

According to these findings, the formation of equiaxed microstructure during the single-pass hybrid laser welding of 25 mm plates in **Paper 3** and Wahba et al. [2016] (Figure 5.5) could be partly attributed to the relatively low or favorable temperature gradients during the solidification of their welds. The

equiaxed solidification mode together with minimal local stresses that is obtained as a result of full penetration welding (Gebhardt et al. [2013]) could have been the main reasons for the absence of solidification cracking in their experiments. The higher stresses in partial penetration welding reported by Gebhardt et al. [2013] could also be confirmed by the results of this study (Farrokhi et al. [2018a]) as the higher local temperature gradients found in the partial penetration welding may result in higher local strains.

Additionally, as has been discussed in **Paper 3**, a favorable convective flow in the full penetration welds could also have supported the grain refinement in such welds. Finally, the general situation that promotes the solidification cracking depending on the penetration-mode, could be speculated according to Figure 5.14.

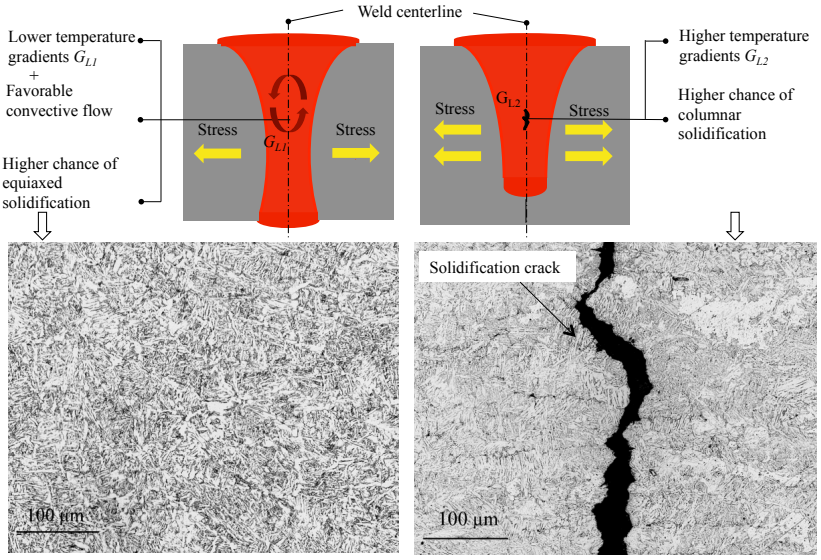

Fig. 5.14: The solidification situation in the weld centerline of full and partial penetration hybrid laser welding of steel and the chance of solidification cracking (Farrokhi et al. [2018a]). The micrographs are from Farrokhi et al. [2017].

5.3 Conclusion and suggestions

5.3.1 Addressing the research objectives

Before closing the chapter, the specific research questions related to the research objective 2 will be answered briefly in this section.

Is it experimentally possible to obtain crack-free welds?

Yes, solidification cracks could be avoided by using single-pass hybrid laser welding on 10 mm thick plates. For the plates with the thickness of 25 mm, Y-grooves were used and the hybrid laser welding was employed only for the root pass. The partial penetration welding experiences in this study were associated with hot cracking.

Using the FE method, based only on thermal conduction, is it possible to model full and partial penetration hybrid laser welding and explain the solidification cracking phenomenon?

Yes, it is possible to model full and partial penetration hybrid laser welding using FE method. For this reason, a special boundary condition is required to account for the different melt flow dynamics that occur during full penetration welding. Therefore, in this study, a double-conical volumetric heat source was developed based on the previously proposed TDC heat source in the literature. Using an adaptive hybrid heat source model that consisted of a double-conical and a double-ellipsoidal heat source, allowed the modeling of the common weld geometries that are obtained by hybrid laser welding of thick-section steels.

This model can be used for the analysis of thermal situations that may contribute to the solidification cracking phenomenon. Moreover, the model can be potentially used as the basis for the calculation of residual stresses after the welding. However, as far as the solidification cracking is concerned, for calculating the local stresses that develop during solidification, a more sophisticated material model is required in order to capture an accurate material response in different phases and temperatures.

What is the influence of penetration-mode on the solidification cracking phenomenon?

In general, the penetration-mode of welding, influences the risk of solidification cracking mainly in two ways: (i) affecting the local stresses that develop during solidification, and (ii) influencing the temperature gradients at the solidification front, and thereby governing the solidification mode. The former has been studied by Gebhardt et al. [2013] and they concluded that the mag-

nitude of tensile stresses in the two crack susceptible regions of laser welds are larger during partial penetration welding compared with the full penetration welding. This could also be confirmed by the results of this study (Farrokhi et al. [2018a]) as the higher local temperature gradients found in the partial penetration welding may result in higher local strains. Concerning the effect of penetration-mode on the solidification mode, the results of this study (Farrokhi et al. [2018a]) suggested that the thermal situation, and thereby the temperature gradients at the solidification front of full penetration welding (compared with partial penetration welding) are more in the favor of equiaxed solidification mode, which is more resistant to solidification cracking.

5.3.2 Suggestions for crack-free welding

Based on the findings of this research, in order to reduce the risk of hot cracking in hybrid laser welding of thick-section steels, partial penetration welding must be avoided whenever possible. Instead, the welding procedure and joint design must provide the possibility of full penetration welding, meaning that no solid metal should remain below the melt at the root side during welding. A few examples of "high risk" and "low risk" weld passes are depicted in Figure 5.15 for a given welding process' parameters.

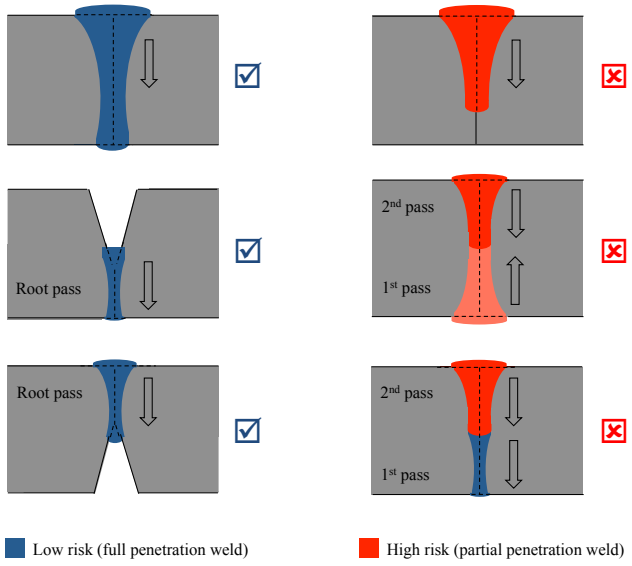

Fig. 5.15: Examples of different hybrid laser weld passes with high and low risks of hot cracking.

Chapter 6

Conclusion

This chapter sums up the general conclusions of this thesis. Further detailed concluding remarks can be found in the corresponding papers in Part III. Finally, the chapter is closed with suggesting a few relevant research subjects for future on the basis of this study.

6.1 Concluding remarks

6.1.1 Research Objective 1

In an integrated laser cutting-welding system: what is the influence of laser cut surface characteristics, such as (i) surface roughness and (ii) cut kerf shape, on the quality and efficiency of the subsequent hybrid laser welding?

To answer this question, a number experiments were carried out and the results were analyzed and reported in **Papers 1-4**. The following general conclusions can be drawn as following:

- An integrated laser cutting-welding system can be used to increase the quality and efficiency of the subsequent hybrid laser welding process, compared with using the conventional machining methods for joint preparation. In addition, such system allows more flexibility during the manufacturing. For instance, in the same cutting unit, it is possible to provide different joint preparations and groove shapes for the subsequent welding process by using simply different cutting parameters and setups.

- In comparison with commercial preparation methods with milling machines, using plates with nitrogen assisted laser cut-edge surface mainly provides three benefits; (i) It is possible to increase the travel speed of the root welding; (ii) It allows welding with zero pre-set gap, which makes it easier to position workpieces. This is because the natural gap caused by the rough striations of the laser cut surface compensates for the lack

of pre-set gap; (iii) Finally, using plates with nitrogen assisted laser cut-edge surface, makes it possible to obtain welds with higher quality and stability at the root side.

- In comparison with commercial preparation methods with milling machines, using plates with nitrogen assisted laser cut-edge surface can provide an acceptable perpendicularity level that has almost no negative effect on the subsequent welding process. Using plates with oxygen assisted laser cut-edge surface may result in highly curved shapes at the edge that reduces the repeatability of the subsequent welding. However, in some cases, the tulip-shape groove enabled an increase in penetration depth and allowed welding of 25 mm plates in single-pass.

6.1.2 Research Objective 2

How is it possible to reduce the chance of solidification cracking in hybrid laser welding of thick-section steels?

To answer this question, the results of experimental observations in **Papers 1-5** were analyzed and some of the experiments were numerically modeled in **Papers 5** and **6**. The following general conclusions can be drawn as following:

- Solidification cracks could be avoided by using single-pass hybrid laser welding on 10 mm thick plates. For the plates with the thickness of 25 mm, Y-grooves were used and the hybrid laser welding was employed only for the root pass. The partial penetration welding experiences in this study were associated with hot cracking. This is evidence to the importance of penetration-mode and the design of joint/groove before welding.

- In general, the penetration-mode of welding, influences the chance of solidification cracking, mainly in two ways: (i) affecting the local stresses that develop during solidification, and (ii) influencing the temperature gradients at the solidification front, and thereby governing the solidification mode. The former has been studied by Gebhardt et al. [2013] and they concluded that the magnitude of tensile stresses in the two crack susceptible regions of laser welds are larger during partial penetration welding compared with the full penetration welding. Concerning the effect of penetration-mode on the solidification mode, the results of this study (Farrokhi et al. [2018a]) suggested that the thermal situation, and thereby the temperature gradients at the solidification front of full penetration welding (compared with partial penetration welding) are more in the favor of equiaxed solidification mode, which is more resistant to solidification cracking.

6.2 Future work

Based on the concluding remarks, some directions for future research can be seen within the two areas of focus in this study.

- **Surface roughness and keyhole stability.** The striations of nitrogen assisted laser cutting in the butt joint of 25 mm thick plates, resulted in higher welding speed and high stability during the subsequent hybrid laser welding. It would be very interesting to perform an in-situ observation of the keyhole characteristics during these experiments using high-speed cameras. According to the mathematical modeling of the laser-keyhole interaction by Kaplan [2012a], even relatively small waviness of the melt surface at the keyhole, can strongly modulate the angles of incidence, and thereby the Fresnel-absorption. It would be so interesting to investigate if the striations of the laser cutting have any influence on the waviness of the melt surface during laser welding. This could possibly explain the increase of efficiency/speed observed in this study as a result of striations on the butt joint of steel.

- **Groove design for single-pass welding.** Using a high-speed laser cutting procedure resulted in the butt joints that had a tulip-shape groove. This special groove, together with the use of backing during welding, enabled an increase in penetration depth and allowed welding of 25 mm plates in single-pass. However, the experiments were not completely repeatable as a result of dimensional variation of the groove due to the unstable cutting process. Although these experiments cannot be used in practice, they suggest the possibility of single-pass welding of 25 mm plates. Therefore, it would be interesting to produce a more simple groove using milling that is based the tulip-shape in these experiments. This may provide the chance of single-pass welding of 25 mm plates without having the instability problem.

- **Calibration of the numerical model.** During the numerical modeling in this study, the calibration was carried out by try and error. A systematic method for calibration of the hybrid model in this study, would facilitate the use of this model in future applications. This is of great importance when it comes to employing such a model in industry. Moreover, due to the complexity of the multi-physical phenomena involved during hybrid laser welding, the prediction of heat distribution is difficult in the fusion zone. Further modifications can be applied in the hybrid heat source model to increase the adaptivity of the model. For instance, the effective energy distribution of the laser in the lower and upper cones (Q_{l1} and Q_{l2}) can be modified to change the laser energy proportions and to obtain a more accurate fit with respect to the experiments.

- **Penetration-mode and residual stresses.** In this study, the numerical model was used only for the calculation of temperature distribution and thermal gradients. However, using the results of temperature data from the same model, it would be possible to calculate the residual stresses as well. It would be very interesting to compare the residual stresses that develop during the full and partial penetration welding experiments.

- **Analysis of the hot cracks.** Although the cracks that were observed in this study could be categorized in two groups in terms of size and location (Figure 5.3), in which they appeared in the laser-dominated region, they exhibited different orientations in some cases. The majority of hot cracks as reported in **Papers 1-4**, was found exactly on the centerline of the laser-dominated region and had an orientation normal to the plate surface (see Figure 5.2 and 5.3). This type of crack exhibited the typical solidification cracking characteristics that is found on the weld centerline of steels, e.g. in Akselsen et al. [2013] . However, in a few cases (Figure 5.6a), hot cracks appeared in a different orientation. Although, in terms of location, they could be classified as Type B cracks, their orientation was perpendicular to the welding direction (in the transverse cross section). These types of hot cracks have also been reported in the literature, e.g. in the laser welds of tempered steel, Schaefer et al. [2015]. However, in this thesis, the time limitation did not allow further microscopic metallography of the cracks. It would be very interesting to analyze these cracks in more details by using e.g. the Scanning Electron Microscopy (SEM) analysis.

- **Hot cracking theories.** Temperature gradient of the solid-liquid interface is one of the most important parameters that has been included in many models and criteria of hot cracking. Using the data presented in this paper, it would be interesting to discuss the increased risk of hot cracking in the partial penetration welding experiments based on the theoretical criteria and models on hot tearing in the literature.

- **Grain refinement practice.** The results of numerical analysis in this study showed that full penetration welding has a higher chance for grain refinement in the weld centerline compared with the partial penetration welding. It would be very interesting to investigate this in practice. For example, comparing the chance of grain refinement in full and partial penetration welding during the mechanical vibration or electro-magnetic grain refinement techniques. Such an experiment would determine the significance of the penetration-mode effect on the chance of grain refinement.

References

Akselsen, O. M., Wiklund, G., Ostby, E., Sorgjard, A., and Kaplan, A. (2013). A first assessment of laser hybrid welding of 420 mpa steel for offshore structure application. In Kaplan, A. F. H. and Engstrom, H., editors, *14th Nordic Laser Materials Processing Conference Nolamp*, pages 171–182. Lulea tekniska universitet.

Apblett, W. and Pellini, W. (1954). Factors which influence weld hot cracking. *Welding Research Supplement*, 33(2):83–90.

Arata, Y., Matsuda, F., and Matsui, A. (1974). Effect of welding condition on solidification structure in weld metal of aluminum alloy sheets. *Transactions of the JWRI*, 3(1):89–97.

Bergström, D., Powell, J., and Kaplan, A. F. (2007). The absorptance of steels to Nd:YLF and Nd:YAG laser light at room temperature. *Applied Surface Science*, 253(11):5017–5028.

Bochvar, A. and Sviderskaya, Z. (1947). [N/A]. *Izv Akad Nauk*, 3:349–355.

Borland, J. (1960). Generalized theory of super-solidus cracking in welds and castings. *Brittish Welding Journal*, 7(8):508–512.

Chen, Y., Feng, J., Li, L., Chang, S., and Ma, G. (2013). Microstructure and mechanical properties of a thick-section high-strength steel welded joint by novel double-sided hybrid fibre laser-arc welding. *Materials Science and Engineering A*, 582:284–293.

Coniglio, N. and Cross, C. E. (2013). Initiation and growth mechanisms for weld solidification cracking. *International Materials Reviews*, 58(7):375–397.

Cross, C. E. (2005). On the Origin of Weld Solidification Cracking. In *Hot Cracking Phenomena in Welds*, pages 3–18. Springer-Verlag.

Cross, C. E. and Böllinghaus, T. (2006). The Effect of Restraint on Weld Solidiflcation Cracking in Aluminium. *Welding in the World*, 50(11-12):51–54.

Dahotre, N. and Harimkar, S. (2008). *Laser fabrication and machining of materials*. Springer Science & Business Media.

Dal, M. and Fabbro, R. (2016). [INVITED] An overview of the state of art in laser welding simulation. *Optics and Laser Technology*, 78:2–14.

Farrokhi, F. (2014). *Autogenous high power fiber laser welding of Optim 960 QC ultra high strength steel, (Master's thesis).* Lappeenranta University of Technology.

Farrokhi, F., Endelt, B., Andersen, R. S., and Kristiansen, M. (2018a). Temperature Gradients at the Solidification Front of Full and Partial Penetration Hybrid Laser Welding. *Submitted to a refereed journal [Under review].*

Farrokhi, F., Endelt, B., and Kristiansen, M. (2018b). A Numerical Model for Full and Partial Penetration Hybrid Laser Welding of Thick-Section Steels. *Submitted to a refereed journal [Under review]*.

Farrokhi, F. and Kristiansen, M. (2016). A practical approach for increasing penetration in hybrid laser-arc welding of steel. *Physics Procedia*, 83:577–586.

Farrokhi, F., Larsen, R. M., and Kristiansen, M. (2017). Single-pass hybrid laser welding of 25 mm thick steel. *Physics Procedia*, 89:49–57.

Farrokhi, F., Nielsen, S. E., Schmidt, R. H., Pedersen, S. S., and Kristiansen, M. (2015a). Effect of Cut Quality on Hybrid Laser Arc Welding of Thick Section Steels. *Physics Procedia*, 78(August):65–73.

Farrokhi, F., Siltanen, J., and Salminen, A. (2015b). Fiber Laser Welding of Direct-Quenched Ultrahigh Strength Steels: Evaluation of Hardness, Tensile Strength, and Toughness Properties at Subzero Temperatures. *Journal of Manufacturing Science and Engineering*, 137(6):061012.

Frostevarg, J. (2018). Factors affecting weld root morphology in laser keyhole welding. *Optics and Lasers in Engineering*, 101:89–98.

Frostevarg, J. and Kaplan, A. F. H. (2014). Undercuts in laser arc hybrid welding. *Physics Procedia*, 56(C):663–672.

Ganaha, T., Pearce, B. P., and Kerr, H. W. (1980). Grain structures in aluminium alloy GTA welds. *Metallurgical Transactions A*, 11(8):1351–1359.

Garland, J. (1974). 21: 121, 1974. *Metal Constuction / British Welding Journal*, 21.

Gebhardt, M. O., Gumenyuk, A., Quiroz Penaranda, V., and Rethmeier, M. (2012). Laser/GMA hybrid welding of thick-walled precision pipes. *Welding and cutting*, 5:312–318.

Gebhardt, M. O., Gumenyuk, A., and Rethmeier, M. (2013). Numerical analysis of hot cracking in laser-hybrid welded tubes. *Advances in Materials Science and Engineering*, 2013.

Gebhardt, M. O., Gumenyuk, a., and Rethmeier, M. (2014). Solidification cracking in laser GMA hybrid welding of thick-walled parts. *Science and Technology of Welding and Joining*, 19(3):209–213.

Goldak, J., Chakravarti, A., and Bibby, M. (1984). A new finite element model for welding heat sources. *Metallurgical Transactions B*, 15(2):299–305.

Gook, S., Gumenyuk, a., and Rethmeier, M. (2014). Hybrid laser arc welding of X80 and X120 steel grade. *Science and Technology of Welding and Joining*, 19(1):15–24.

Goppold, C., Zenger, K., Herwig, P., Wetzig, A., Mahrle, A., and Beyer, E. (2014). Experimental analysis for improvements of process efficiency and cut edge quality of fusion cutting with 1 micro-meter laser radiation. *Physics Procedia*, 56:892–900.

Haug, P., Rominger, V., Speker, N., Weber, R., Graf, T., Weigl, M., and Schmidt, M. (2013). Influence of laser wavelength on melt bath dynamics and resulting seam quality at welding of thick plates. *Physics Procedia*, 41:49–58.

Hojerslev, C. (2013). Welding of Thick Walled Steel Components With 32 kW Laser Power. In *The 14th Nordic Laser Materials Processing Conference*, pages 391–397, Gothenburg. Lulea University of Technology.

Hondros, E. and Seah, M. (1977). Segregation to interfaces. *International Metals Reviews*, 22(1):262–301.

Honore, M. and Hojerslev, C. (2013). 32 kW Disc-Laser System Delivering up to 2x16 kW in A Common Melt Pool. In *The 14th Nordic Laser Materials Processing Conference*, pages 399–408, Gothenburg. Lulea University of Technology.

HYBLAS (2003). Economical and safe laser hybrid welding of structural steel, Contract No RFSR-CT-2003-00010.

Ivarson, A. (2017). Influence of laser type on cutting mild and AR steels [Industrial presentation]. In *16th Nordic Laser Materials Processing Conference, NOLAMP16*, Aalborg.

Kaldellis, J. K., Apostolou, D., Kapsali, M., and Kondili, E. (2016). Environmental and social footprint of offshore wind energy. Comparison with onshore counterpart. *Renewable Energy*, 92:543–556.

Kannengiesser, T. and Kromm, A. (2007). Design-Specific Influences in Local Weld Displacement and Hot Cracking. In *International Conference on Welding and Joining of Materials*, Peru.

Kaplan, A. F. H. (2012a). Fresnel absorption of 1 micrometer and 10 micrometer laser beams at the keyhole wall during laser beam welding: Comparison between smooth and wavy surfaces. *Applied Surface Science*, 258(8):3354–3363.

Kaplan, A. F. H. (2012b). Local absorptivity modulation of a 1 micro-meter-laser beam through surface waviness. *Applied Surface Science*, 258(24):9732–9736.

Katayama, S. (2009). Fundamentals of hybrid laser-arc welding. In Olsen, F. O., editor, *Hybrid Laser-Arc Welding*, pages 28–46. Woodhead Publishing Limited.

Kou, S. (2003). *Welding Metallurgy*. John Wiley & Sons, 2nd edition.

Kou, S. (2015). A criterion for cracking during solidification. *Acta Materialia*, 88:366–374.

Kou, S. and Le, Y. (1988). Welding parameters and the grain structure of weld metal - A thermodynamic consideration. *Metallurgical Transactions A*, 19(4):1075–1082.

Kristensen, J. K. (2009). Quality control and assessing weld quality in hybrid laser-arc welding. In Olsen, F. O., editor, *Hybrid Laser-Arc Welding*, pages 127–139. Woodhead Publishing Limited.

Kristiansen, M. (2014). Project Meeting Presentation. Technical report, Aalborg University.

Kristiansen, M., Farrokhi, F., Kristiansen, E., and Villumsen, S. (2017). Application of hybrid laser arc welding for the joining of large offshore steel foundations. *Physics Procedia*, 89:197–204.

Kristiansen, M., Selchau, J., Olsen, F. O., and Hansen, K. S. (2013). Quality and Performance of Laser Cutting with a High Power SM Fiber Laser. In *Proceedings of the 14th NOLAMP conference*, pages 109–120, Gothenburg. Lulea University of Technology.

Kurz, W., Bezencon, C., and Gaumann, M. (2001). Columnar to equiaxed transition in solidification processing. *Science and Technology of Advanced Materials*, 2(1):185–191.

Lan, H., Wang, W., Shangguan, Y., and Lin, S. (2011). Fundamental studies on high power fiber laser cutting performance of 30 mm thick carbon steel plate. *Proceedings of 2011 6th International Forum on Strategic Technology*, 1:6–11.

Lancaster, J. (1999). *The Metallurgy of Welding*. Abington Publishing, 6th edition.

Lawrence, J. and Li, L. (2018). The Challenges Ahead for Laser Macro, Micro and Nano Manufacturing. In Lawrence, J., editor, *Advances in Laser Materials Processing: Technology, Research and Applications (Woodhead Publishing Series in Welding and Other Joining Technologies)*. Elsevier Ltd.

Lindgren, L. E. (2006). Numerical modelling of welding. *Computer Methods in Applied Mechanics and Engineering*, 195(48-49):6710–6736.

Lippold, J. C. (2015). *Welding metallurgy and weldability*. John Wiley & Sons.

LSTC (2015). *LS-DYNA keyword user's manual, volume I*.

LSTC (2017). *LS-DYNA Theory Manual*.

Mackwood, A. P. and Crafer, R. C. (2005). Thermal modelling of laser welding and related processes: A literature review. *Optics and Laser Technology*, 37(2):99–115.

Mahrle, a. and Beyer, E. (2009). Theoretical aspects of fibre laser cutting. *Journal of Physics D: Applied Physics*, 42:175507(9pp).

Matsuda, F. (1990). Solidification crack susceptibility of weld metal. In David, S. and Vitek, J., editors, *Recent Trends in Welding Science and Technology*, pages 127–136. ASM International.

Matsuda, F., Nakagawa, H., and Sorada, K. (1982). Dynamic observation of solidification and solidification cracking during welding with optical microscope. *Transactions of JWRI*, 11(2):67–77.

Medovar, B. (1954). On the nature of weld hot cracking. *Avtomaticheskaya Svarka*, 7(4):12–28.

Moeslund, T. B. (2012). *Introduction to Video and Image Processing: Building Real Systems and Applications*. Springer-Verlag.

Mohandas, T., Reddy, G. M., and Madhusudhan Reddy, G. (1997). A comparison of continuous and pulse current gas tungsten arc welds of an ultra high strength steel. *Journal of Materials Processing Technology*, 69(1-3):222–226.

Morren, J. and de Haan, S. W. H. (2005). Ridethrough of wind turbines with doubly-fed induction generator during a voltage dip. *IEEE Transactions on Energy Conversion*, 20(2):435–441.

Nielsen, S. A. (2014a). Project Meeting Presentation. Technical report, Universal Foundation.

Nielsen, S. E. (2014b). Project Meeting Presentation. Technical report, Force Technology.

Nielsen, S. E. (2015). High Power Laser Hybrid Welding - Challenges and Perspectives. *Physics Procedia*, 78(August):24–34.

N.Nguyen, A.Ohta, K.Matsuoka, N.Suzuki, and Y.Maeda (1999). Analytical Solutions for Transient Temperature of Semi-Infinite Body Subjected to 3-D Moving Heat Sources. *Welding Research Supplement*, I(August):265–274.

Norman, A. F., Ducharme, R., Mackwood, A., Kapadia, P., and Prangnell, P. B. (1998). Application of thermal modelling to laser beam welding of aluminium alloys. *Science and Technology of Welding & Joining*, 3(5):260–266.

Olsen, F. O., editor (2009). *Hybrid Laser-Arc Welding*. Woodhead Publishing Limited.

Orishich, A. M., Malikov, A. G., Shulyatyev, V. B., and Golyshev, A. A. (2014). Experimental comparison of laser cutting of steel with fiber and CO2 lasers on the basis of minimal roughness. *Physics Procedia*, 56:875–884.

Pearce, B. P. and Kerr, H. W. (1981). Grain refinement in magnetically stirred GTA welds of aluminum alloys. *Metallurgical Transactions B*, 12(3):479–486.

Pellini, W. (1952). Strain theory of hot tearing. *Foundry*, 80:124–133.

Petring, D., Molitor, T., Schneider, F., and Wolf, N. (2012). Diagnostics, Modeling and Simulation: Three Keys Towards Mastering the Cutting Process with Fiber, Disk and Diode Lasers. *Physics Procedia*, 39:186–196.

Pocorni, J., Petring, D., Powell, J., Deichsel, E., and Kaplan, A. (2014). Differences in Cutting Efficiency between CO2 and Fiber Lasers when Cutting Mild and Stainless Steels. In *33rd International Congress on Applications of Lasers and Electro-Optics (ICALEO)*, page paper #905. LIA.

Pocorni, J., Powell, J., Ilar, T., Schwarz, A., and Kaplan, A. F. H. (2013). Measuring the state-of-the-art in laser cut quality. In Kaplan, A. and Engstrom, H., editors, *Proceedings of the 14th NOLAMP conference*, pages 101–108, Gothenburg. Lulea University of Technology.

Poprawe, R., Schulz, W., and Schmitt, R. (2010). Hydrodynamics of material removal by melt expulsion: Perspectives of laser cutting and drilling. *Physics Procedia*, 5:1–18.

Porter, D. A., Easterling, K. E., and Sherif, M. Y. (2009). *Phase Transformations in Metals and Alloys*. CRC Press, 3rd editio edition.

Powell, J., Ilar, T., Frostevarg, J., Torkamany, M. J., Na, S.-J., Petring, D., Zhang, L., and Kaplan, A. F. H. (2015). Weld root instabilities in fiber laser welding. *Journal of Laser Applications*, 27(S2):S29008.

Prokhorov, N. and Prokhorov, N. (1971). Fundamentals of the theory for technological strength of metals while crystallising during welding. *Transactions of JWRI*, 2(2):205–213.

Pumphrey, W. and Jennings, P. (1948). A Consideration of the Nature of brittleness at Temperatures Above the Solidus in Castings and Welds in Aluminum Alloys. *Journal of the Institute of Metals*, 75:235–256.

Rao, B. and Nath, A. (2002). Melt flow characteristics in gas-assisted laser cutting. *Sadhana - Academy Proceedings in Engineering Sciences*, 27:569–575.

Rao, Z. H., Liao, S. M., and Tsai, H. L. (2011). Modelling of hybrid laser-GMA welding: review and challenges. *Science and Technology of Welding and Joining*, 16(4):300–305.

Rappaz, M., Drezet, J., and Gremaud, M. (1999). A new hot-tearing criterion. *Metallurgical and Materials Transactions A*, 30(2):449–455.

Reddy, G. M. and Mohandas, T. (2001). Explorative studies on grain refinement of ferritic stainless steel welds. *Journal of Materials Science Letters*, 20(8):721–723.

Reisgen, U., Olschok, S., Jakobs, S., Schleser, M., Mokrov, O., and Rossiter, E. (2012). Laser Beam Submerged Arc Hybrid Welding. *Physics Procedia*, 39:75–83.

Rethmeier, M., Sergej, G., Marco, L., and Andrey, G. (2009). Laser-Hybrid Welding of Thick Plates up to 32 mm Using a 20 kW Fibre Laser. *Quarterly journal of the Japan welding society*, 27(2):74–79.

Rutter, J. and Chalmers, B. (1953). A prismatic substructure formed during solidification of metals. *Canadian Journal of Physics*, 31(1):15–39.

Schaefer, M., Kessler, S., Scheible, P., Speker, N., and Harrer, T. (2017). Hot cracking during laser welding of steel: influence of the welding parameters and prevention of cracks. In Kaierle, S., editor, *Proceedings of SPIE*, volume 10097, pages 100970E1–8. SPIE.

Schaefer, M., Speker, N., Weber, R., Harrer, T., and Graf, T. (2015). Lasers in Manufacturing Conference 2015 Analysing Hot Crack Formation in Laser Welding of Tempered Steel. *Lasers in Manufacturing Conference 2015*, 1.

Schempp, P., Cross, C. E., Pittner, A., Oder, G., Neumann, R. S., Rooch, H., Dörfel, I., Österle, W., and Rethmeier, M. (2014a). Solidification of GTA aluminum weld metal: Part I - Grain morphology dependent upon alloy composition and grain refiner content. *Welding Journal*, 93(2):53s–59s.

Schempp, P., Cross, C. E., Pittner, A., and Rethmeier, M. (2014b). Solidification of GTA aluminum weld metal: Part 2 - Thermal conditions and model for columnar-to-equiaxed transition. *Welding Journal*, 93(3):69s–77s.

Scintilla, L. D., Tricarico, L., Wetzig, A., Mahrle, A., and Beyer, E. (2011). Primary losses in disk and CO2 laser beam inert gas fusion cutting. *Journal of Materials Processing Technology*, 211:2050–2061.

Snyder, B. and Kaiser, M. J. (2009). Ecological and economic cost-benefit analysis of offshore wind energy. *Renewable Energy*, 34(6):1567–1578.

Sokolov, M., Salminen, A., Katayama, S., and Kawahito, Y. (2015). Reduced pressure laser welding of thick section structural steel. *Journal of Materials Processing Technology*, 219:278–285.

Sokolov, M., Salminen, A., Somonov, V., and Kaplan, A. F. H. (2012). Laser welding of structural steels: Influence of the edge roughness level. *Optics and Laser Technology*, 44(7):2054–2071.

Steen, W. M. and Mazumder, J. (2010). *Laser Material Processing*. Springer-Verlag, 4th edition.

Stelzer, S., Mahrle, A., Wetzig, A., and Beyer, E. (2013). Experimental investigations on fusion cutting stainless steel with fiber and CO2 laser beams. *Physics Procedia*, 41:399–404.

Tani, G., Tomesani, L., and Campana, G. (2003). Prediction of melt geometry in laser cutting. *Applied Surface Science*, 208-209:142–147.

Toropov, V. (1957). On the mechanism of hot cracking of welds. *Metallo Obra Metallov*, 6:54–58.

Tsukamoto, S., Zhao, L., Sugino, T., and Arakane, G. (2008). Distribution of Wire Feeding Elements in Laser-arc Hybrid Welds. In *Laser Materials Processing Conference (ICALEO)*, pages 498–505. LIA.

Victor, B. M. (2011). Hybrid Laser Arc Welding. *ASM Handbook*, 6A(2011):321 – 328.

Villafuerte, J. C. and Kerr, H. W. (1990). Electromagnetic stirring and grain refinement in stainless-steel GTA welds. *Welding Journal*, 69(1):1–13.

Villafuerte, J. C., Kerr, H. W., and David, S. A. (1995). Mechanisms of equiaxed grain formation in ferritic stainless steel gas tungsten arc welds. *Materials Science and Engineering A*, 194(2):187–191.

Villafuerte, J. C., Pardo, E., and Kerr, H. W. (1990). The effect of alloy composition and welding conditions on columnar-equiaxed transitions in ferritic stainless steel gas-tungsten arc welds. *Metallurgical and Materials Transactions A*, 21(7):2009–2019.

Vollertsen, F., Grunenwald, S., Rethmeier, M., Gumenyuk, A., Reisgen, U., and Olschok, S. (2010). Welding Thick Steel Plates with Fibre Lasers and GMAW. *Welding in the World*, 54(3-4):R62–R70.

Wahba, M., Mizutani, M., and Katayama, S. (2016). Single pass hybrid laser-arc welding of 25 mm thick square groove butt joints. *Materials and Design*, 97(May):1–6.

Wandera, C. and Kujanpaa, V. (2011). Optimization parmeeters for fiblre laser cutting of a 10 mm stainless steel plate. *Proceedings of the Institution of Mechanical Engineers, Part B: Journal of Engineering Manufacture*, 225:641.

Wandera, C., Kujanpaa, V., and Salminen, A. (2011). Laser power requirement for cutting thick-section steel and effects of processing parameters on mild steel cut quality. *Proceedings of the Institution of Mechanical Engineers, Part B: Journal of Engineering Manufacture*, 225:651.

Webster, S., Kristensen, J. K., and Petring, D. (2008). Joining of thick section steels using hybrid laser welding. *Ironmaking & Steelmaking*, 35(7):496–504.

Wu, C., Wang, H. G., and Zhang, Y. M. (2006). A new heat source model for keyhole plasma arc welding in FEM analysis of the temperature profile. *Welding Journal*, 85(12):284–291.

Yilbas, B. S. (2008). Laser cutting of thick sheet metals: Effects of cutting parameters on kerf size variations. *Journal of Materials Processing Technology*, 201(1):285–290.

Yilbas, B.S., Abdul Aleem, B. (2006). Dross formation during laser cutting process. *Journal of Physics D: Applied Physics*, 39:1451–1461.

Yudin, P. V., Zaitsev, A. V., Kovalev, O. B., and Ermolaev, G. V. (2014). Fundamental study of CO2- and fiber laser cutting of steel plates with high speed visualization technique. In *8th International Conference on Photonic Technologies LANE*, page 042004. Bayerisches Laserzentrum GmbH.

Zacharia, T. (1994). Dynamic Stresses in Weld Metal Hot Cracking. *Welding Journal*, 73(July):164s–172s.

Zacharia, T. and Aramayo, G. (1993). Modelling of thermal stresses in welds. In *International Conference Proceedings on Modelling and Control of Joining Processes*, pages 533–540, Orlando, Florida.

Zaitsev, A. V. and Ermolaev, G. V. (2014). Combustion effects in laser-oxygen cutting: Basic assumptions, numerical simulation and high speed visualization. *Physics Procedia*, 56:865–874.

Zareie Rajani, H. R. and Phillion, A. B. (2016). 3-Multi-Scale Modeling of Deformation Within the Weld Mushy Zone. *Materials and Design*, 94:536–545.

Part III

Papers

Paper 1

Effect of Cut Quality on Hybrid Laser Arc Welding of Thick Section Steels

Farhang Farrokhi, Steen E. Nielsen, Rasmus H. Schmidt, Simon S. Pedersen, and Morten Kristiansen

The paper has been published in
Physics Procedia (2015), 15th Nordic Laser Materials Processing Conference,
Vol. 78, pp. 65-73, 2015.

Paper 2

A Practical Approach for Increasing Penetration in Hybrid Laser-Arc Welding of Steel

Farhang Farrokhi and Morten Kristiansen

The paper has been published in
Physics Procedia (2016), 9th International Conference on Photonic Technologies, Vol. 83, pp. 577-586, 2016.

Paper 3

Single-Pass Hybrid Laser Welding of 25 mm Thick Steel

Farhang Farrokhi, Raino M. Larsen, and Morten Kristiansen

The paper has been published in
Physics Procedia (2017), 16th Nordic Laser Materials Processing Conference,
Vol. 89, pp. 49-57, 2017.

Paper 4

Application of Hybrid Laser Arc Welding for the Joining of Large Offshore Steel Foundations

Morten Kristiansen, Farhang Farrokhi, Ewa Kristiansen, and Sigurd Villumsen

The paper has been published in
Physics Procedia (2017), 16th Nordic Laser Materials Processing Conference,
Vol. 89, pp. 197-204, 2017.

Paper 5

A Numerical Model for Full and Partial Penetration Hybrid Laser Welding of Thick-Section Steels

Farhang Farrokhi, Benny Endelt, and Morten Kristiansen

The paper has been submitted to a peer-reviewed journal [under review] 2018.

Paper 6

Temperature Gradients at the Solidification Front of Deep Hybrid Laser Welds

Farhang Farrokhi, Benny Endelt, Rasmus S. Andersen and Morten Kristiansen

The paper has been submitted to a peer-reviewed journal [under review] 2018.

Additional Papers

Paper 7

Fiber Laser Welding of Direct-Quenched Ultrahigh Strength Steels: Evaluation of Hardness, Tensile Strength, and Toughness Properties at Subzero Temperatures

Farhang Farrokhi, Jukka Siltanen, and Antti Salminen

The paper has been published in
Journal of Manufacturing Science and Engineering: Transactions of the ASME, Vol. 137(6), pp. 061012, 2015.

Paper 8

Effect of Optical Parameters on Fiber Laser Welding of Ultrahigh Strength Steels and Weld Mechanical Properties at Subzero Temperatures

Antti Salminen, Farhang Farrokhi, Anna Unt, and Ilkka Poutiainen

The paper has been published in
Journal of Laser Applications, Vol. 28(2), pp. 022415, 2016.

Paper 9

For Hybrid Laser Svejsning Kan Tildannelsen af Svejsefugens Overflade Væsentligt Øge Svejsehastigheden

Morten Kristiansen, Sigurd Villumsen, and Farhang Farrokhi

The paper has been published in
Svejsning, Vol. 44(3), pp. 10-14, June 2017.

This thesis ends here.

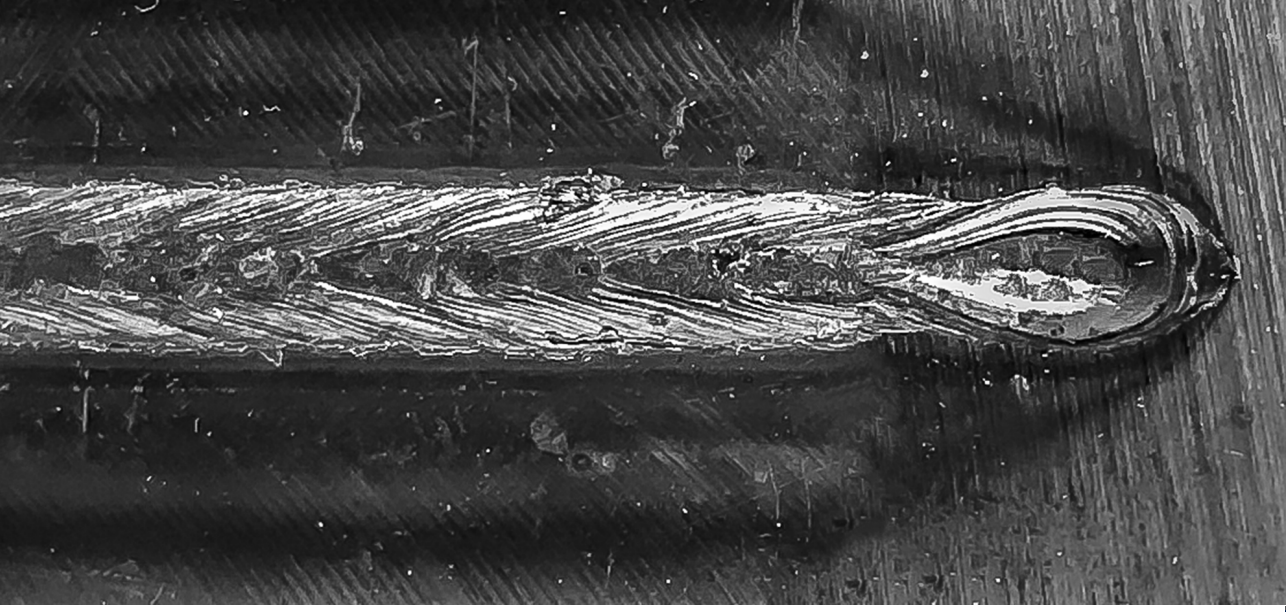

SUMMARY

Manufacturing of large steel structures requires the processing of thick-section steels. Welding is one of the main processes during the manufacturing of such structures and includes a significant part of the production costs. One of the ways to reduce the production costs is to use the hybrid laser welding technology instead of the conventional arc welding methods. However, hybrid laser welding is a complicated process that involves several complex physical phenomena that are highly coupled. Understanding of the process is very important for obtaining quality welds in an efficient way.

This thesis investigates two different challenges related to the hybrid laser welding of thick-section steel plates. Employing empirical and analytical approaches, this thesis attempts to provide further knowledge towards obtaining quality welds in the manufacturing of large steel structures.

ISSN (online): 2446-1636
ISBN (online): 978-87-7210-163-7

AALBORG **UNIVERSITY PRESS**